Neutron Scattering in Spherical Proportional Counters: Investigation of the Experimental Design

Julia Fock

Universität Hamburg
DER FORSCHUNG | DER LEHRE | DER BILDUNG

Spherical Proportional Counters

- Gaseous detector for rare-event detection (such as detection of WIMPs)
- Grounded metallic sphere filled with gas surrounding small anode
- Anode is supported by a rod that supplies high voltage and serves as signal readout
- Interaction produces ionized particles and free electrons
- Gas multiplication in the avalanche region
- Sensitive to low-energy nuclear recoils
- Key parameter: quenching factor
  - Ratio of ionization signal to actual recoil energy
  - Crucial for interpreting nuclear recoil signals
  - Can be measured with neutron scattering in SPCs

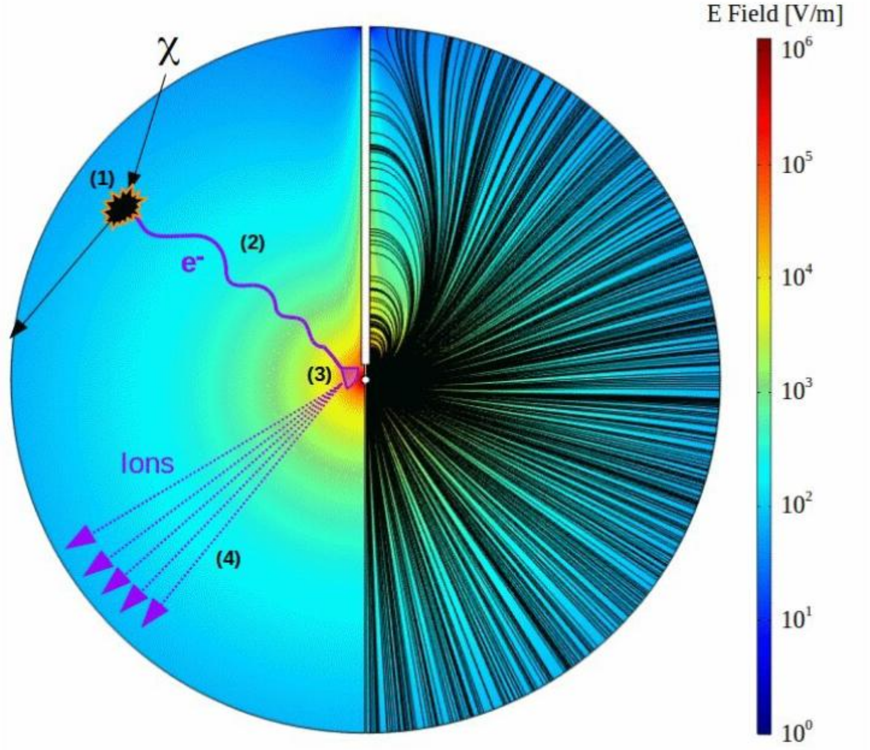

Neutron Scattering in SPCs

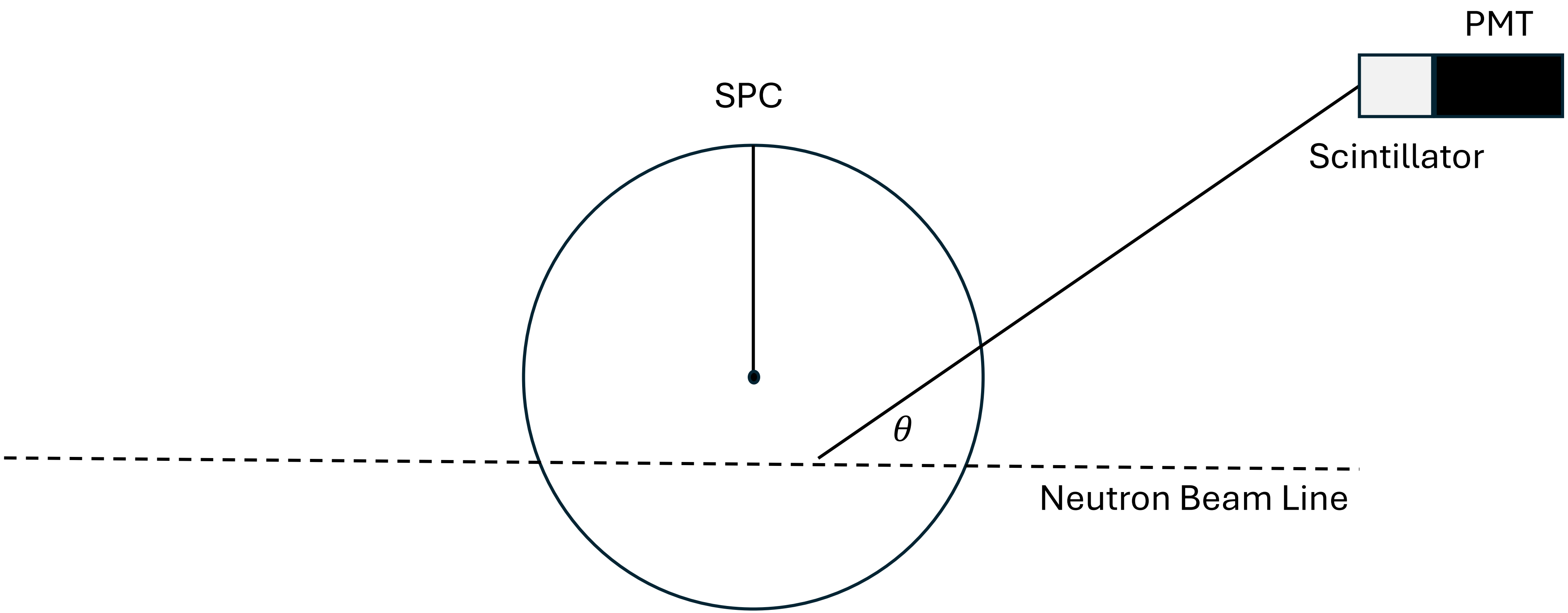

Neutron Scattering in SPCs

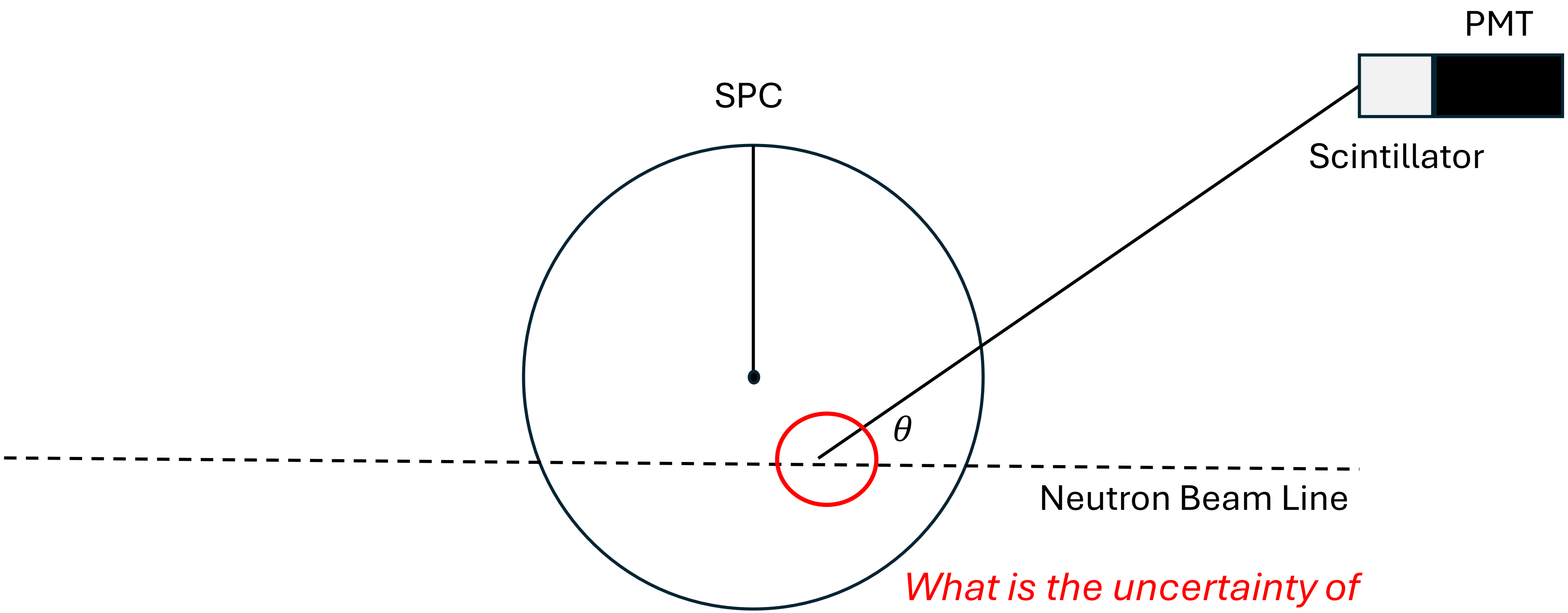

What is the uncertainty of the nuclear recoil energy?

Neutron Scattering Experiment

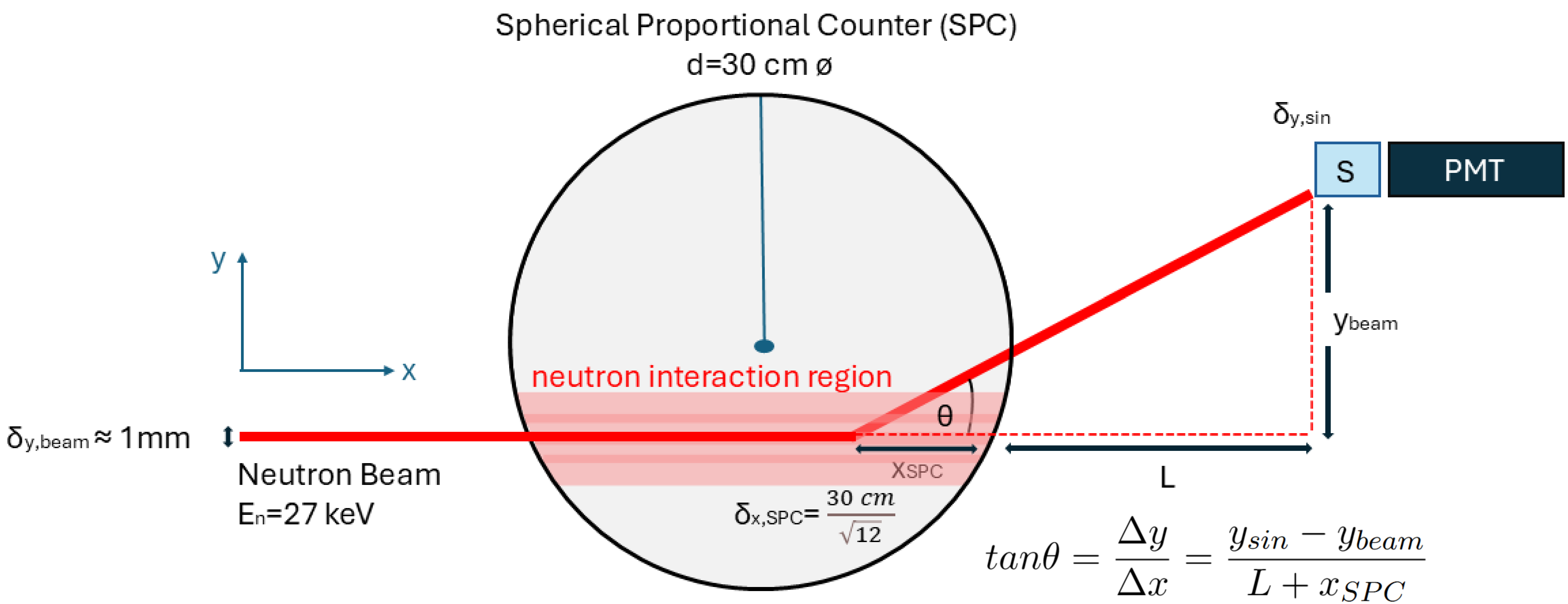

$$tan\theta = \frac{\Delta y}{\Delta x} = \frac{y_{sin} - y_{beam}}{L + x_{SPC}}$$

$$\delta\theta = \frac{cos^2\theta}{L}\sqrt{\delta^2_{y,sin} + \delta^2_{y,beam} + tan^2\theta \cdot \delta^2_{x,SPC}}$$

Scattering Angle for given Nuclear Recoil Energy

$$E_{nr}(\theta, E_n) = 2E_n \frac{M_n^2}{(M_n + M_T)^2} \times \left(\frac{M_T}{M_n} + sin^2\theta - cos\theta \sqrt{(\frac{M_T}{M_n})^2 - sin^2\theta} \right)$$

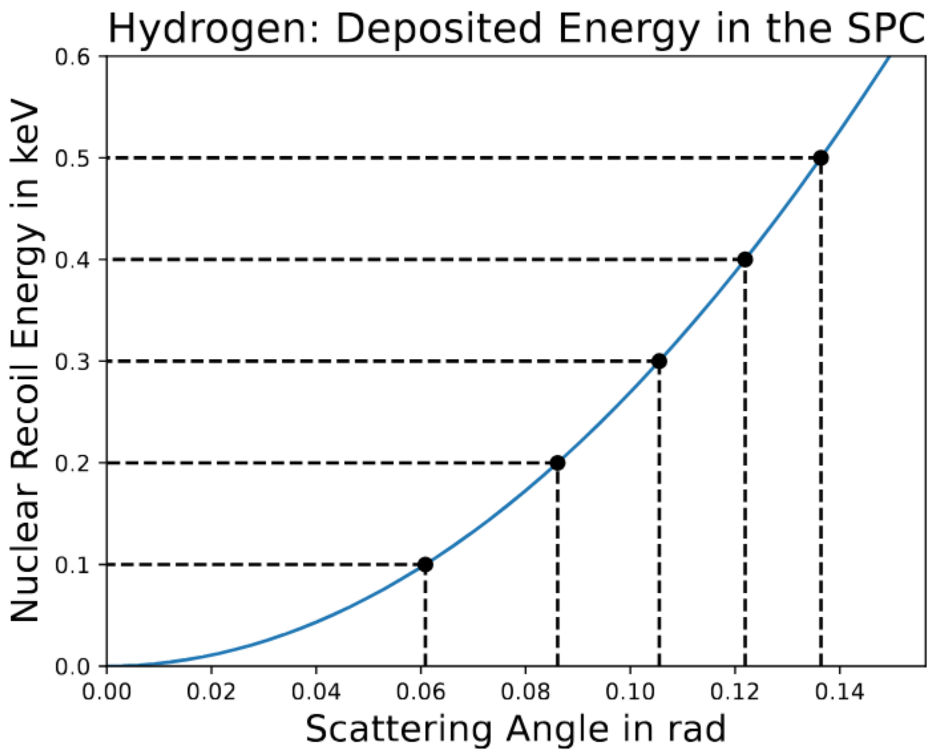

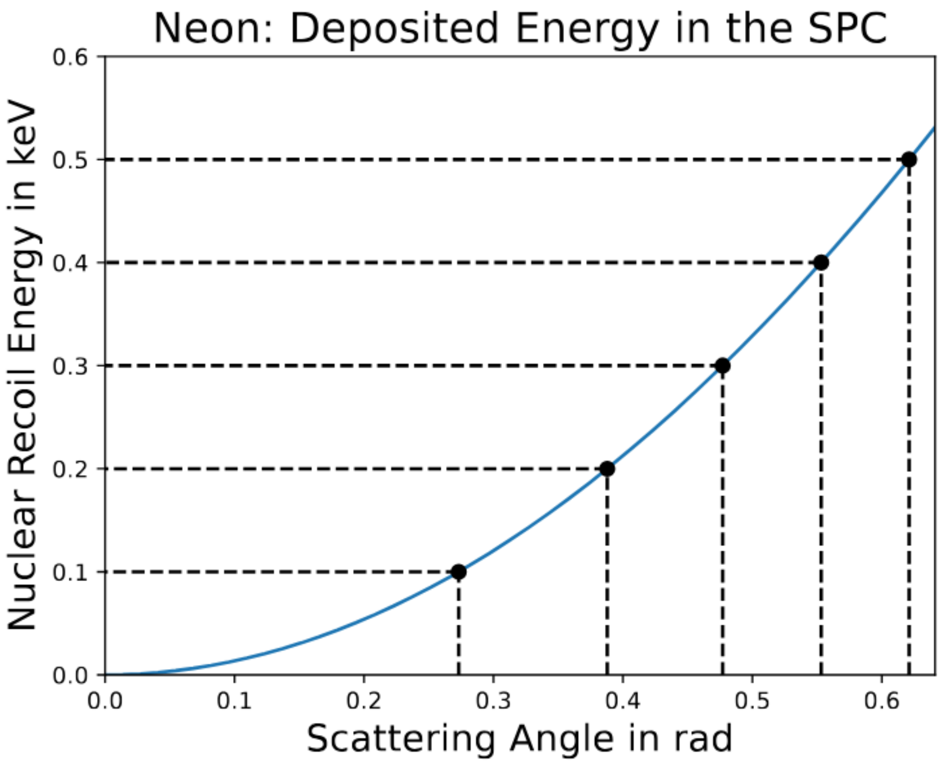

Hydrogen: Uncertainty for $+\delta\theta$

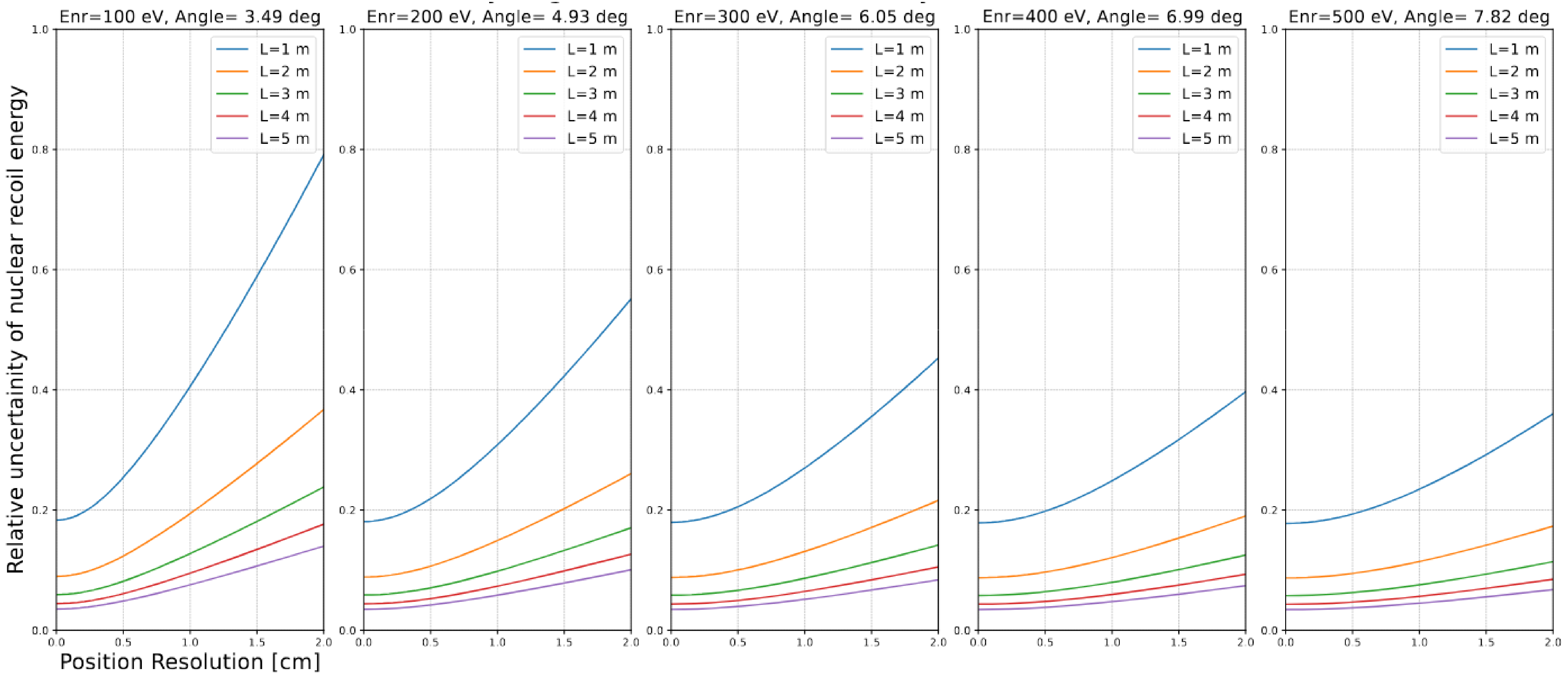

Hydrogen: Uncertainty for -$\delta\theta$

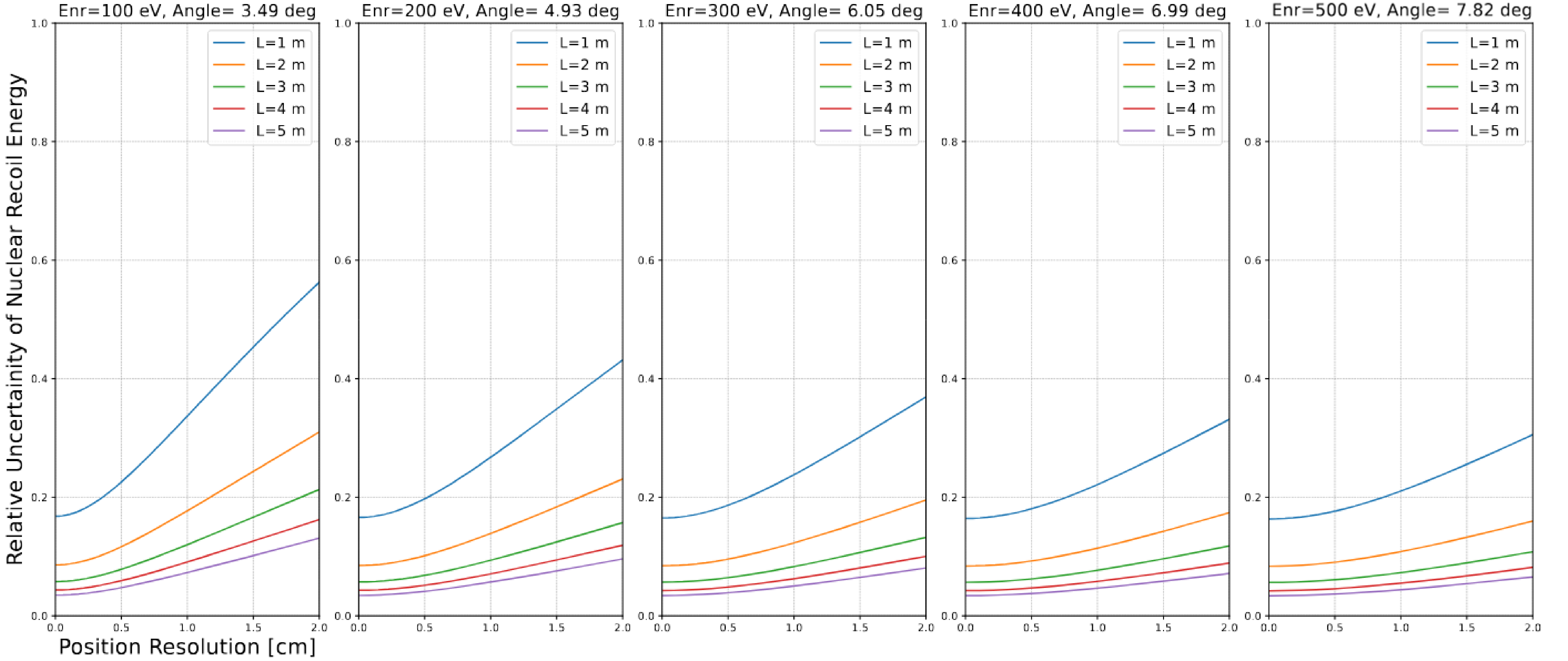

Comparison: Hydrogen and Neon

Hydrogen: $+\delta\theta$

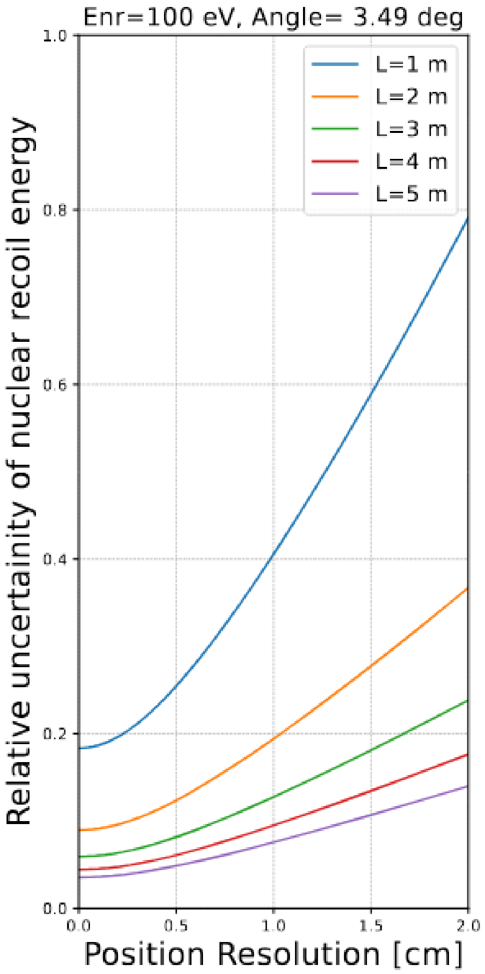

Hydrogen: $-\delta\theta$

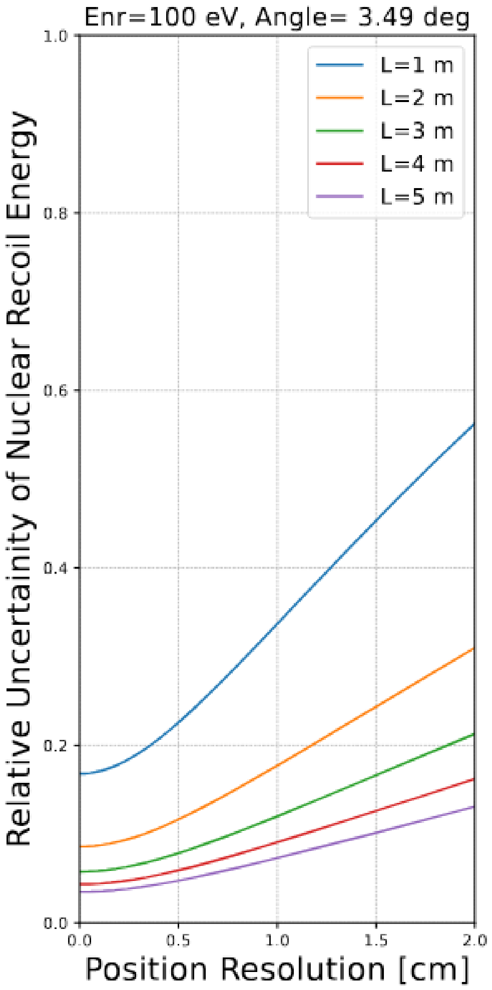

Neon: $-\delta\theta$

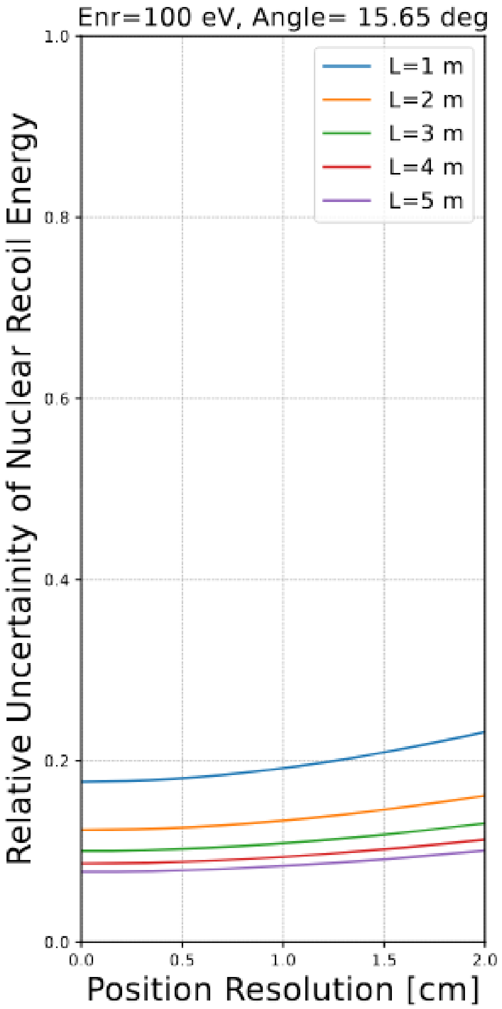

Neon: $-\delta\theta$

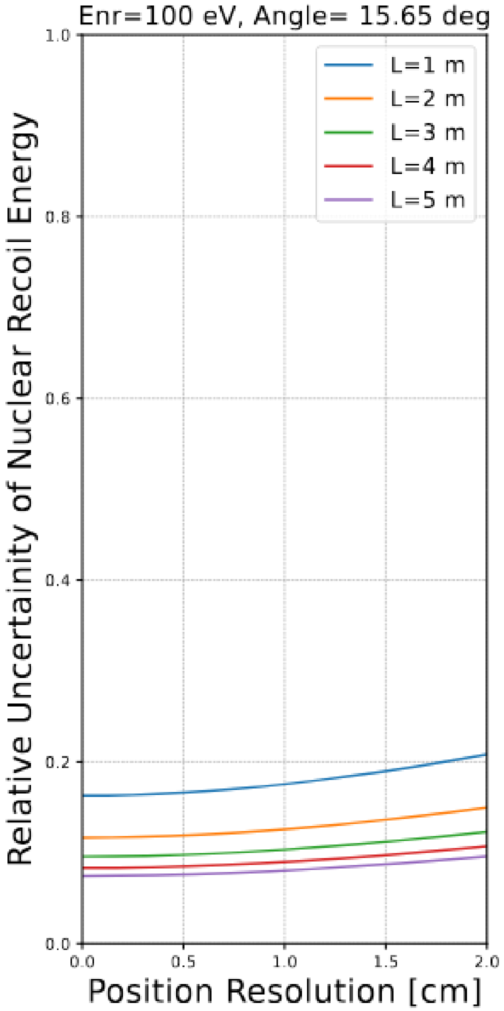

Neutron Scattering in SPCs

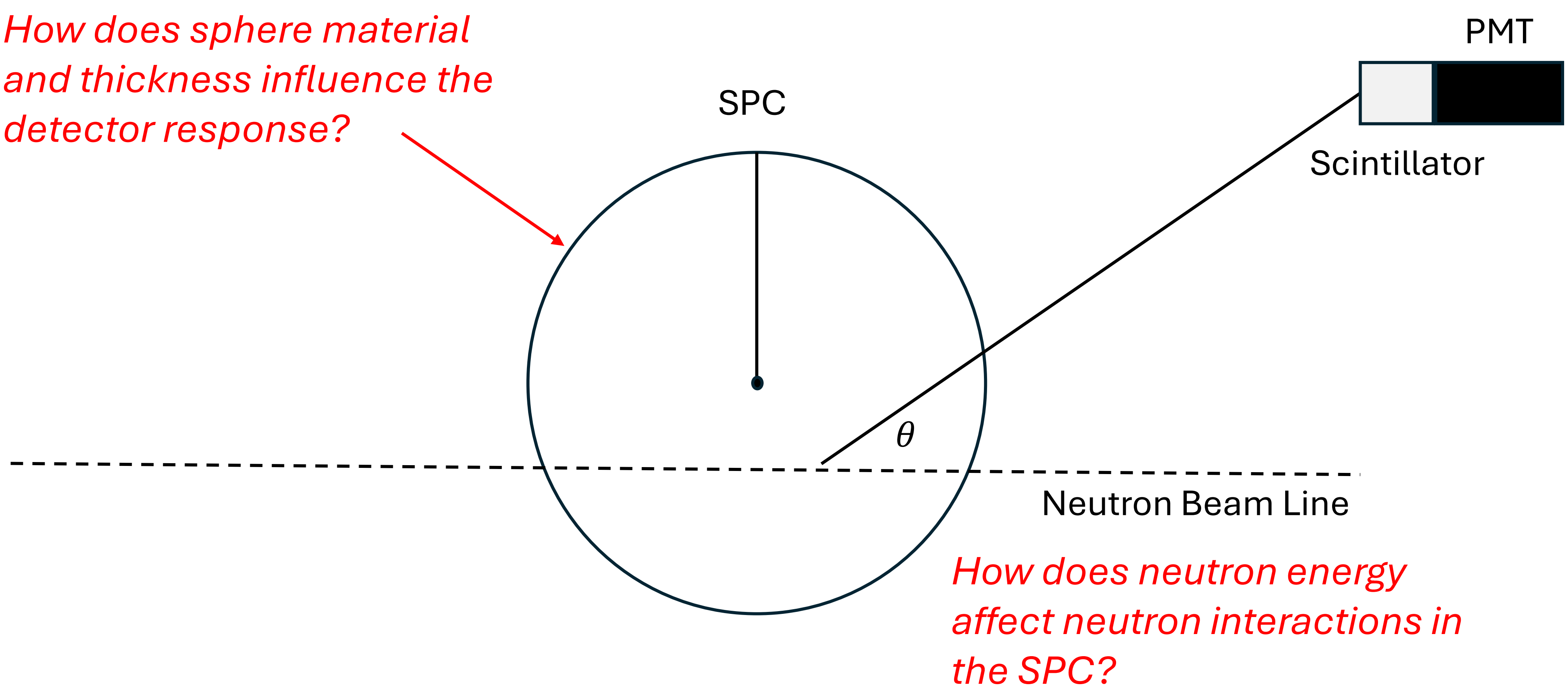

Simulation Setup

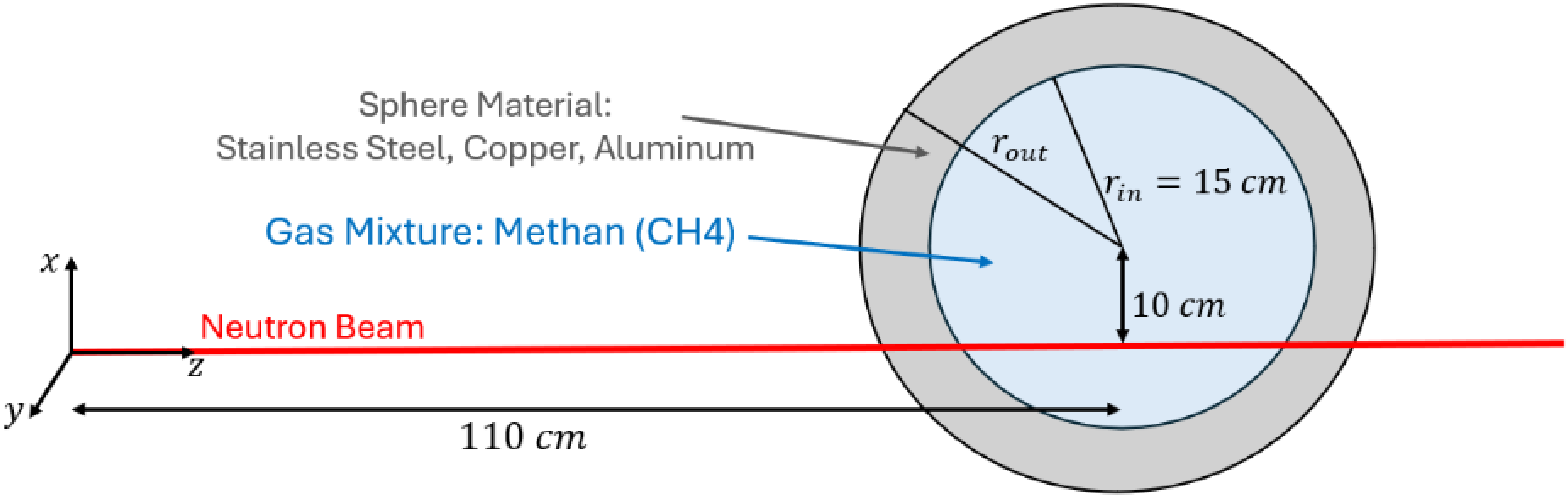

Energy Deposition in the Gas

- Energy deposition in the sphere due to secondary processes from neutron interactions
- Simulation with one million neutrons and a sphere thickness of 1cm
- Energy deposition broadly distributed within the range of the incident neutron energy, indicating elastic scattering interactions

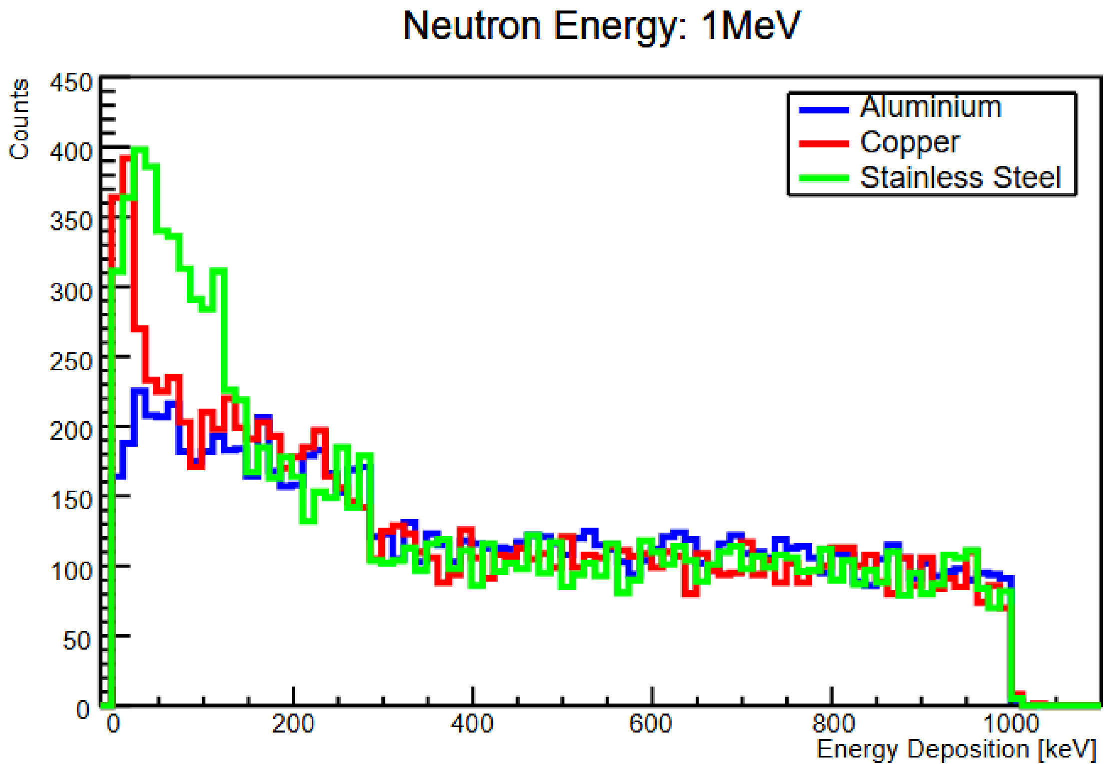

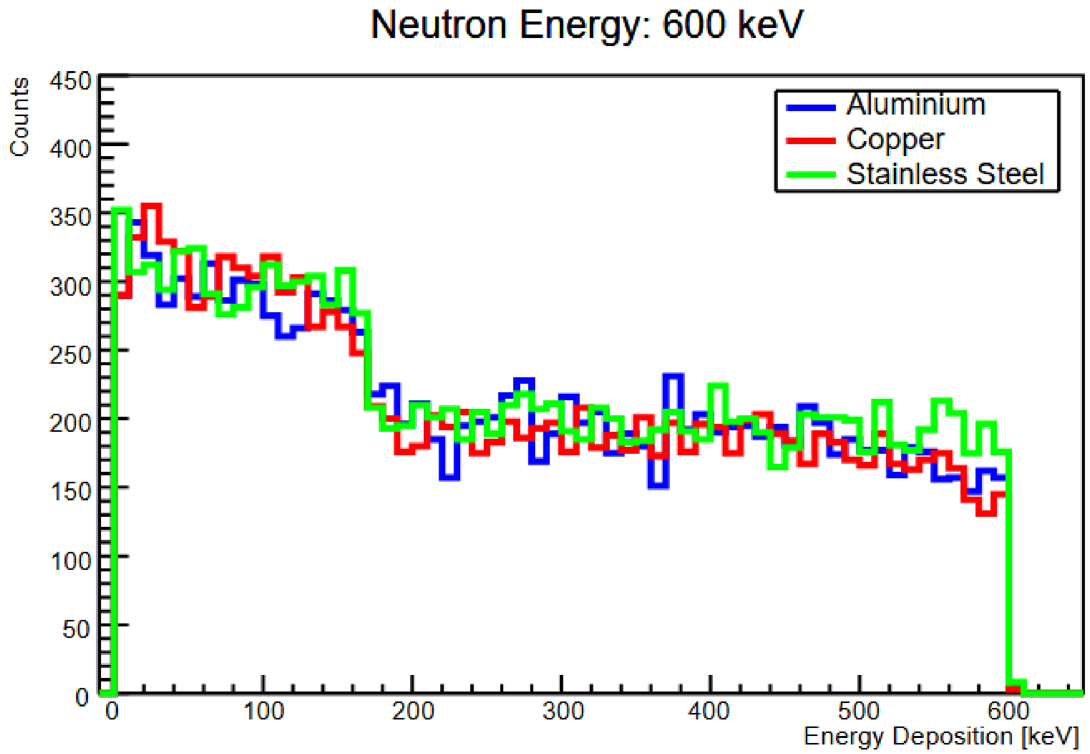

Energy Deposition in the Gas

- Energy deposition in the sphere due to secondary processes from neutron interactions
- Simulation with one million neutrons and a sphere thickness of 1cm
- Energy deposition broadly distributed within the range of the incident neutron energy
- Material influences energy deposition in the gas -> Interactions in the shell material

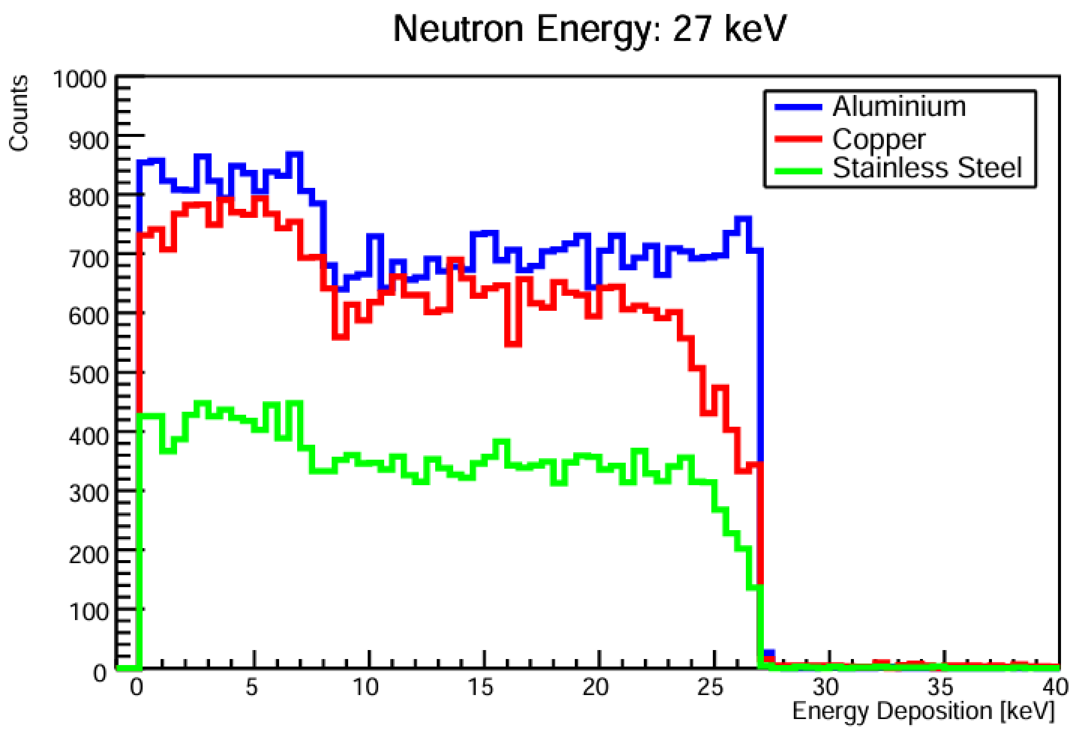

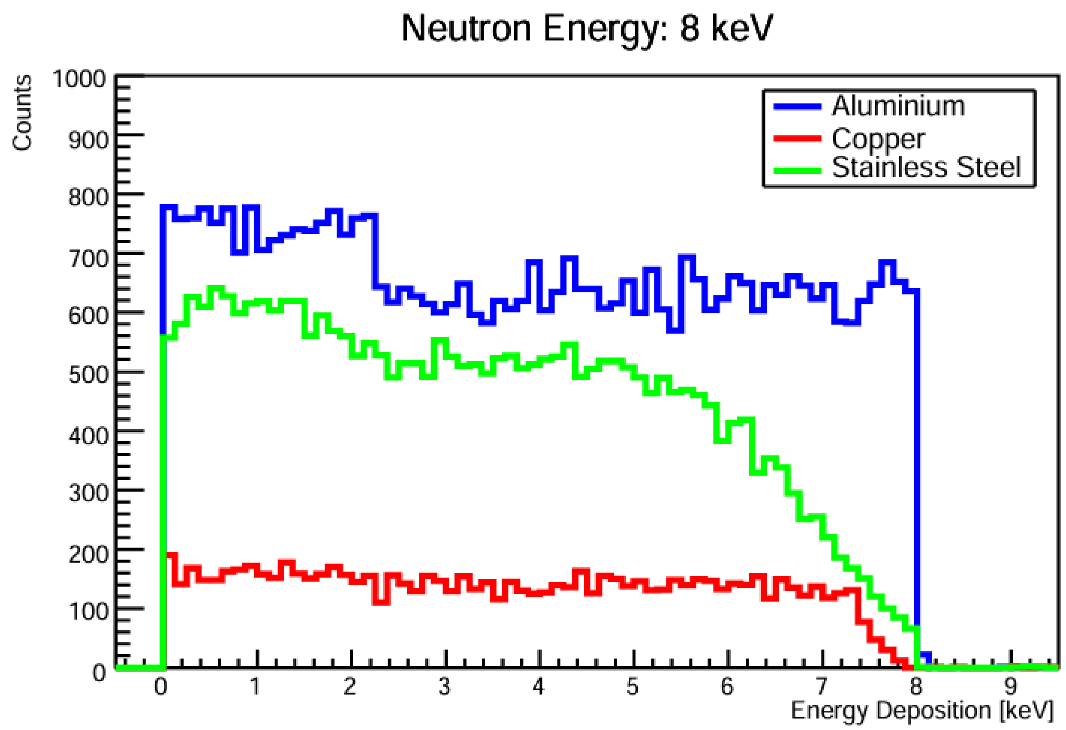

Energy Deposition in the Gas

- Energy deposition in the sphere due to secondary processes from neutron interactions
- Simulation with one million neutrons and a sphere thickness of 1cm
- Deposit significantly more energy in the detector than their initial kinetic energy, indicating inelastic interactions in the shell material

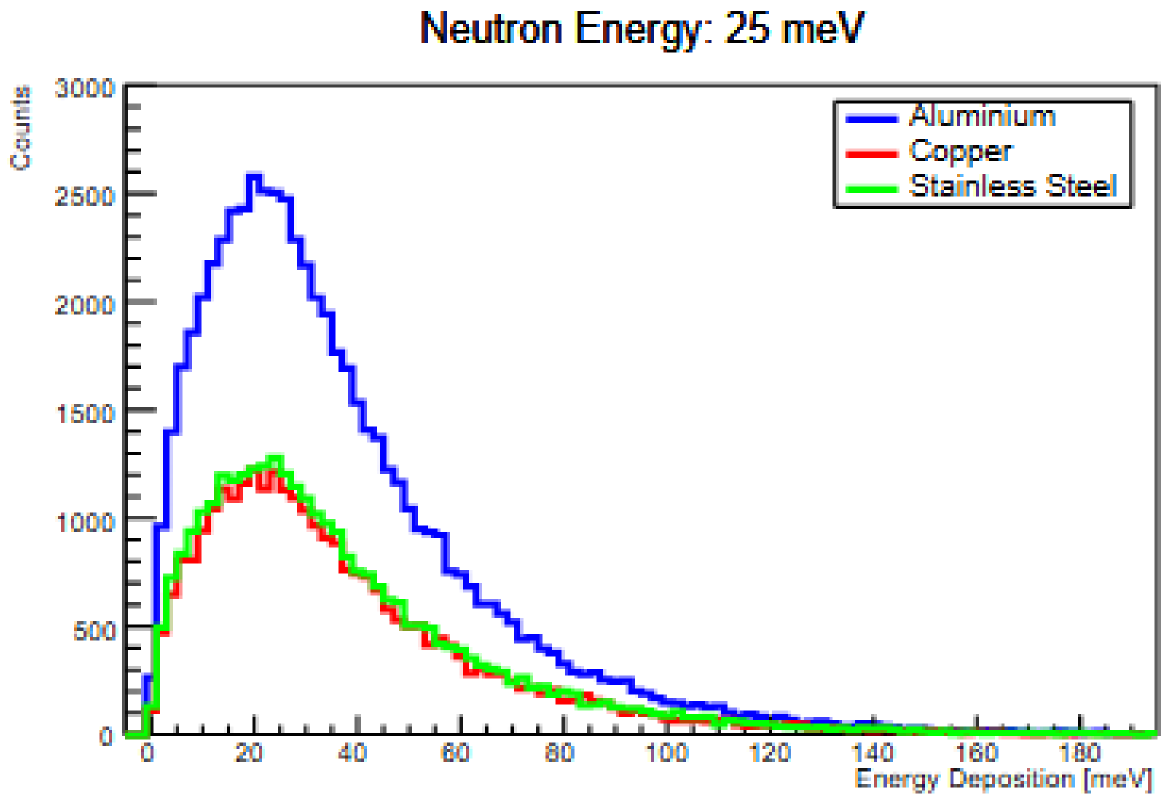

Neutron Interaction Cross-Section

<u>Elastic scattering cross-section:</u>

- Low cross-section for thermal neutrons
- Strong oscillation in the mid-keV range
- Overall lower cross-section for aluminum

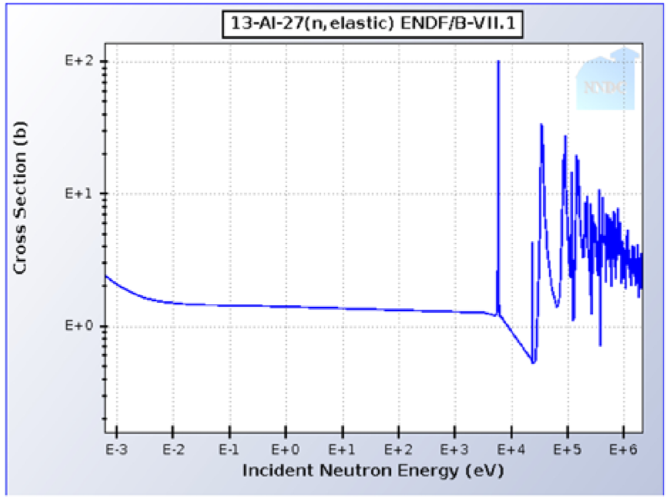

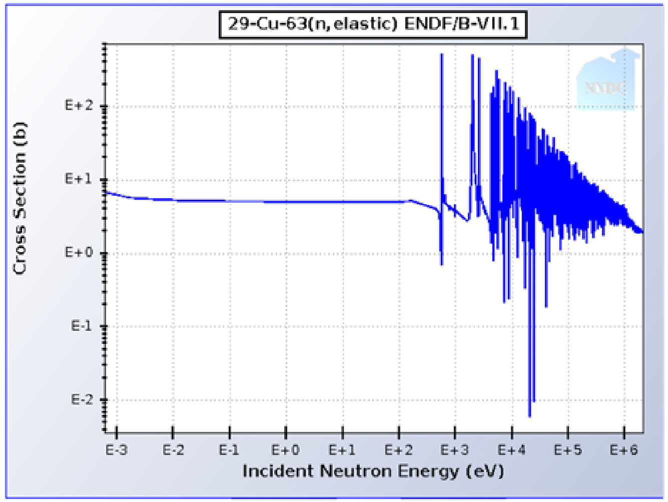

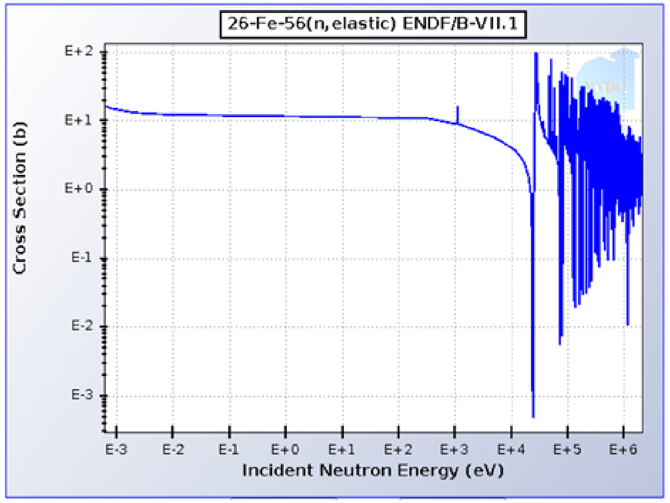

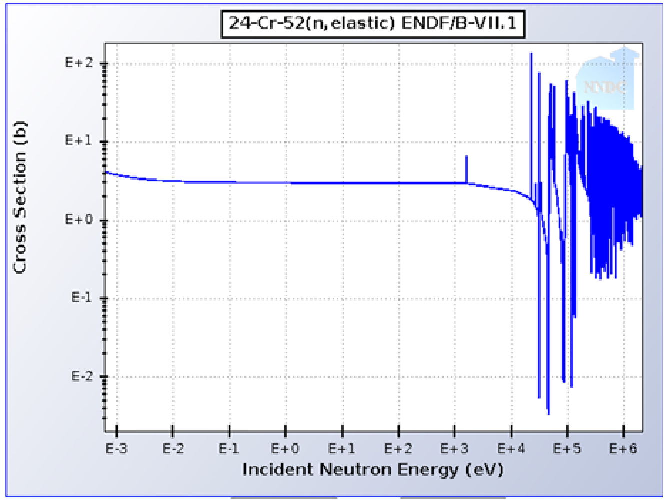

Neutron Interaction Cross-Section

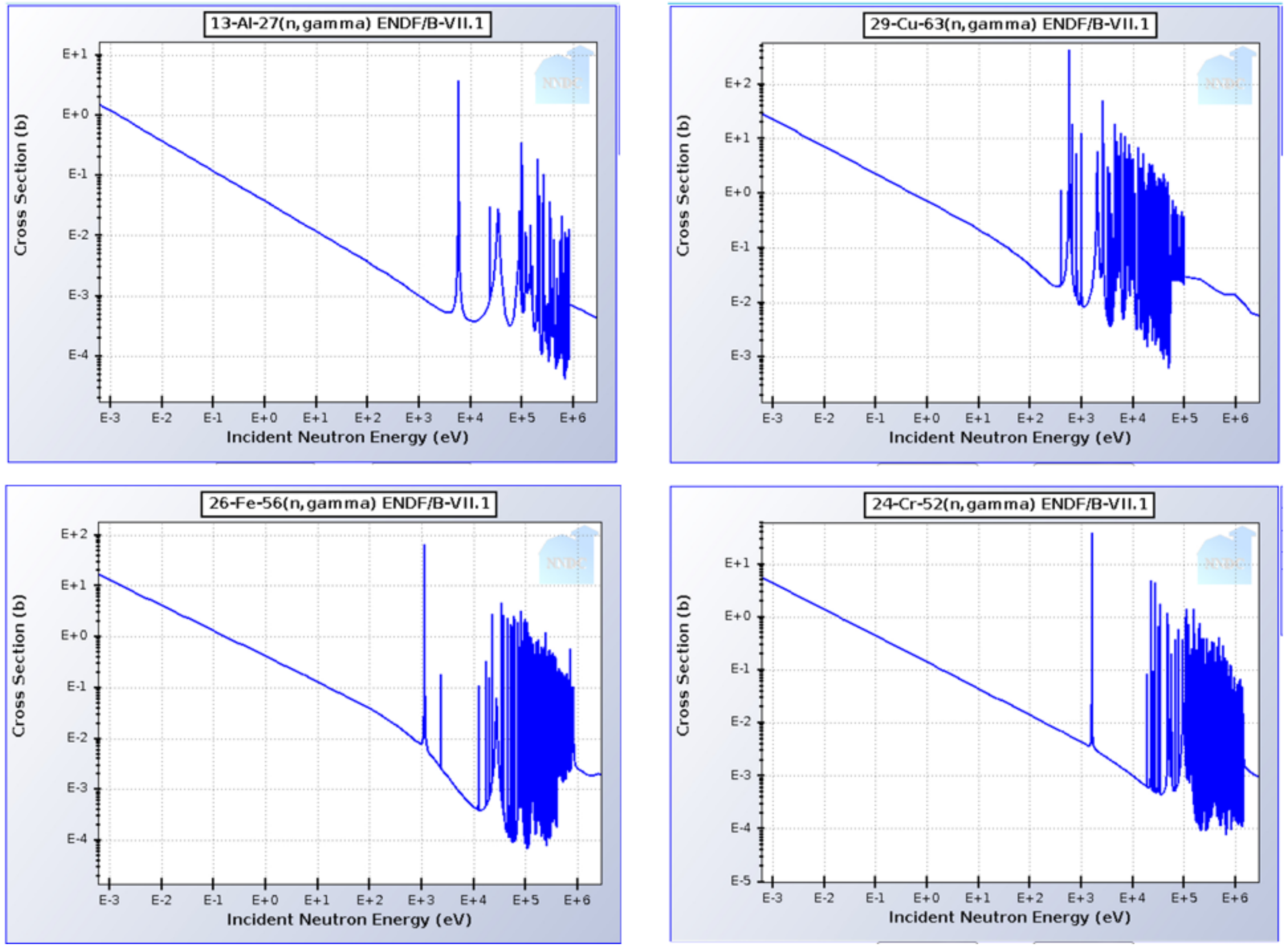

<u>Elastic scattering cross-section:</u>

- Low cross-section for thermal neutrons
- Strong oscillation in the mid-keV range
- Overall lower cross-section for aluminium

<u>Neutron capture cross-section:</u>

- Cross-section rises with lower neutron energy
- Aluminium shows lowest cross-section in the thermal energy range
- Strong oscillation in the mid-keV range

Categorization of Neutron Interactions

- 1eV threshold to exclude low-energy events
- Group interaction scenarios into four distinct cases, based on where and how often the neutron interacted:

1. The neutron only interacted in the gas
2. The neutron only interacted in the shell
3. The neutron interacted first in the gas and then in the shell
4. The neutron interacted first in the shell and then in the gas

Categorization of Neutron Interactions

Copper shell (1 cm)				
Neutron Energy	Only in Gas [%]	Only in Shell [%]	First Gas then Shell [%]	First Shell then Gas [%]
25 meV	1.27±0.08	96.59±0.14	1.27±0.08	0.85±0.07
8 keV	0.07±0.03	5.85±0.24	0.04±0.02	94.04±0.25
27 keV	19.16±0.21	1.06±0.06	25.06±0.23	54.72±0.27
600 keV	35.06±0.42	1.33±0.10	29.07±0.40	34.54±0.42
1 MeV	39.46±0.47	8.89±0.28	27.86±0.43	23.79±0.41

Stainless Steel shell (1 cm)				
Neutron Energy	Only in Gas [%]	Only in Shell [%]	First Gas then Shell [%]	First Shell then Gas [%]
25 meV	1.70±0.12	95.63±0.19	0.85±0.09	1.81±0.12
8 keV	3.31±0.10	0.66±0.05	8.17±0.16	87.87±0.19
27 keV	11.43±0.23	1.55±0.09	13.39±0.25	73.63±0.32
600 keV	55.97±0.43	0.43±0.06	32.40±0.40	11.48±0.27
1 MeV	48.35±0.47	15.57±0.34	23.09±0.40	12.99±0.32

Categorization of Neutron Interactions

Aluminum shell (1 cm)				
Neutron Energy	Only in Gas [%]	Only in Shell [%]	First Gas then Shell [%]	First Shell then Gas [%]
25 meV	16.80±0.59	80.60±0.62	1.92±0.22	0.64±0.13
8 keV	83.94±0.18	0.02±0.01	5.43±0.11	10.61±0.15
27 keV	89.52±0.15	0.06±0.01	7.47±0.13	2.95±0.09
600 keV	56.47±0.43	0.02±0.01	23.43±0.37	20.08±0.35
1 MeV	62.65±0.47	1.27±0.11	23.21±0.41	12.88±0.33

Relative number of absorbed neutrons in the detector shell [%]			
Neutron Energy	Aluminum	Copper	Stainless Steel
25 meV	9.10±0.05	67.08±0.05	57.45±0.05
8 keV	0.02±0.001	2.45±0.02	0.65±0.01
27 keV	0.07±0.01	1.20±0.01	1.16±0.01
600 keV	0.01±0.001	0.62±0.01	1.77±0.02
1 MeV	1.75±0.02	8.29±0.03	22.97±0.06

Study of Neutron Interactions

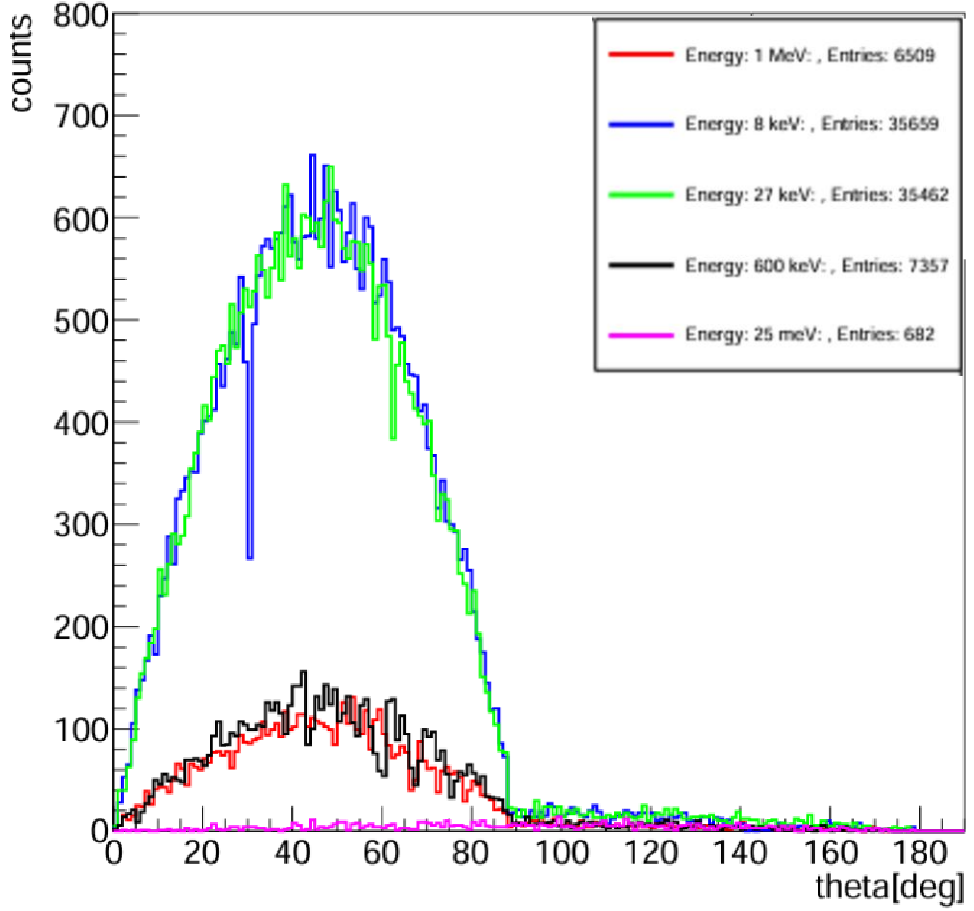

Scattering angle for interactions only in the gas

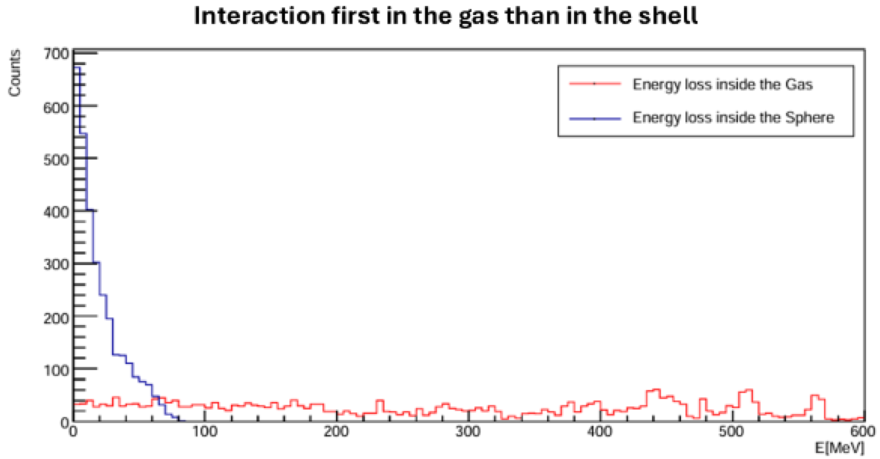

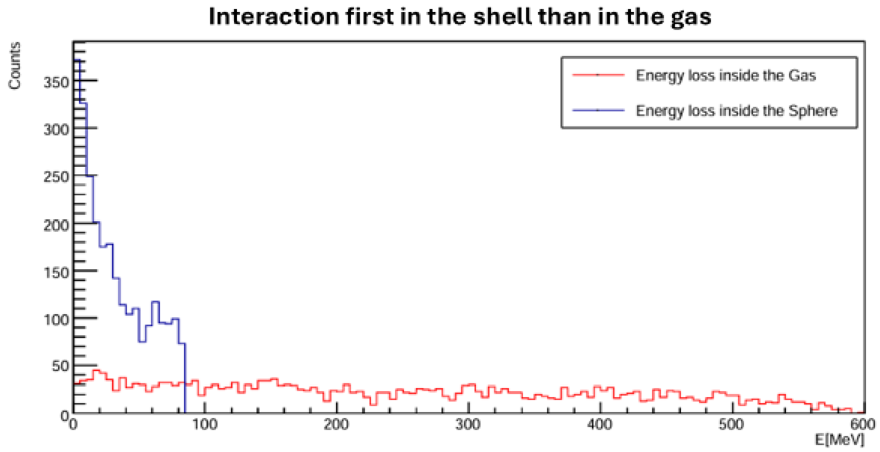

Energy loss for interactions in the sphere gas and shell for 1cm aluminum

Contribution of the Sphere Thickness

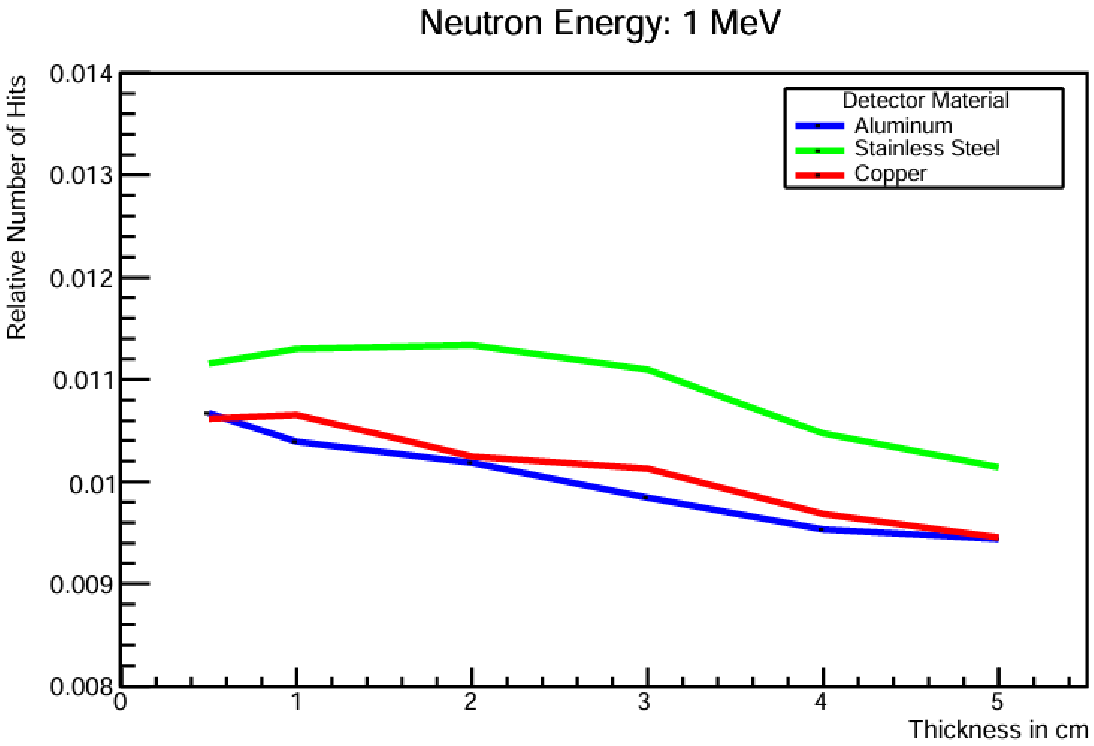

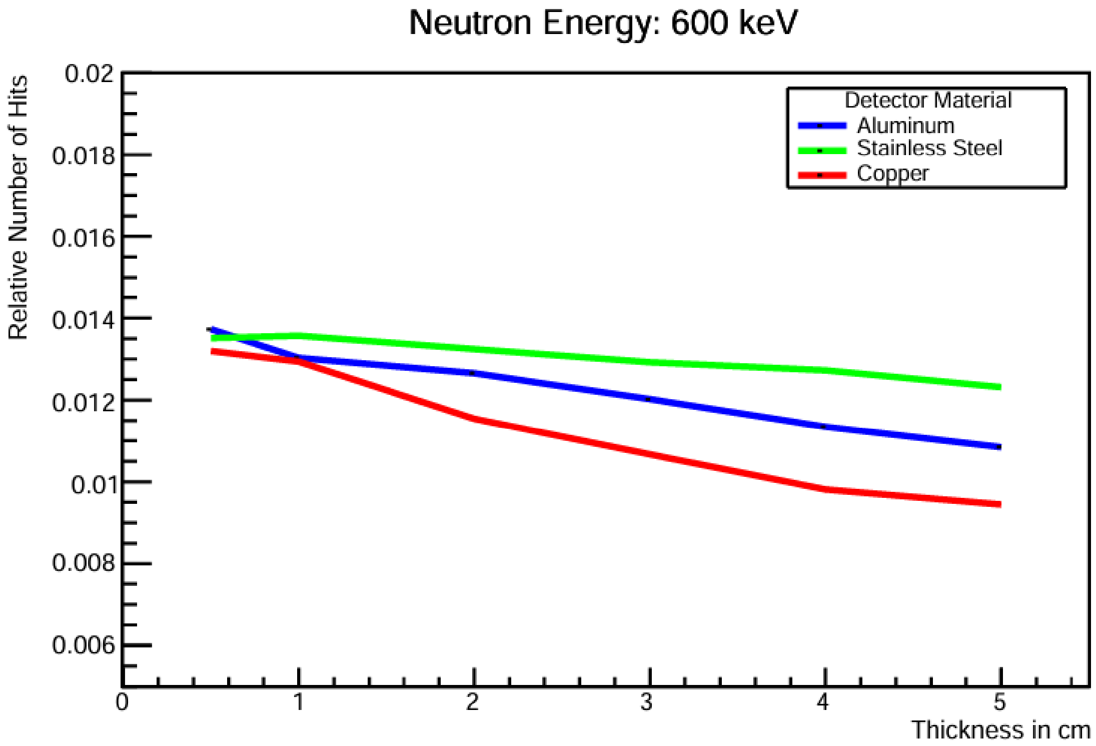

Contribution of the Sphere Thickness

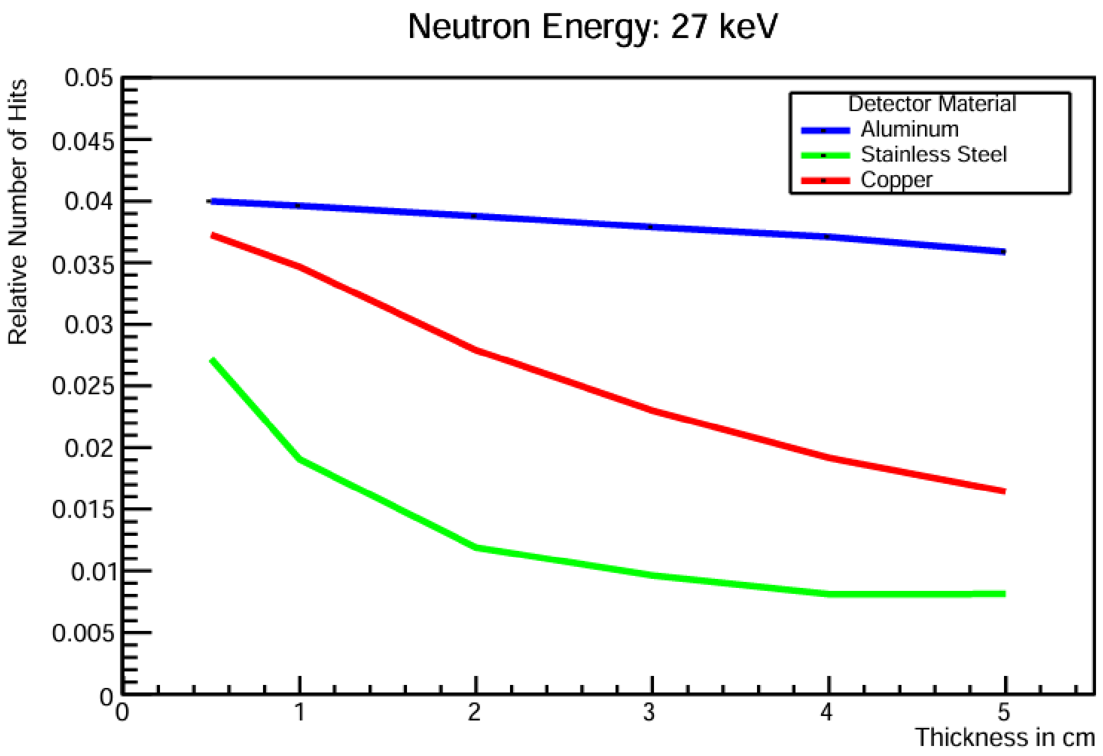

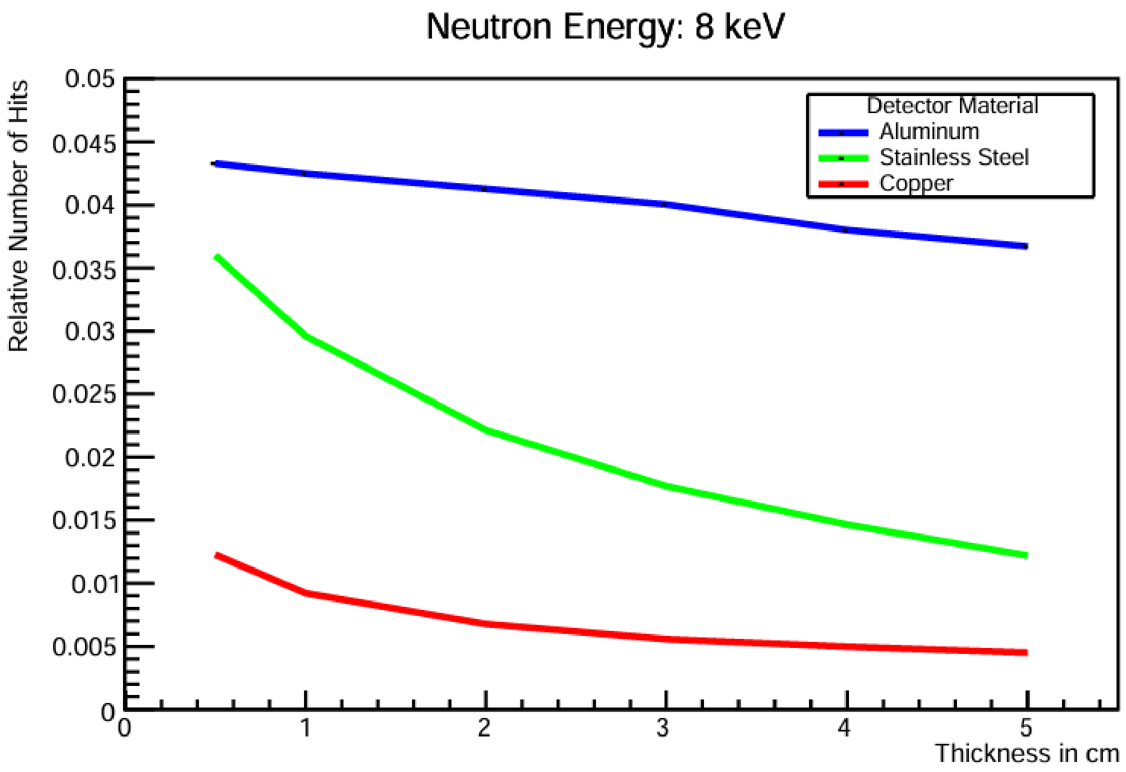

Contribution of the Sphere Thickness

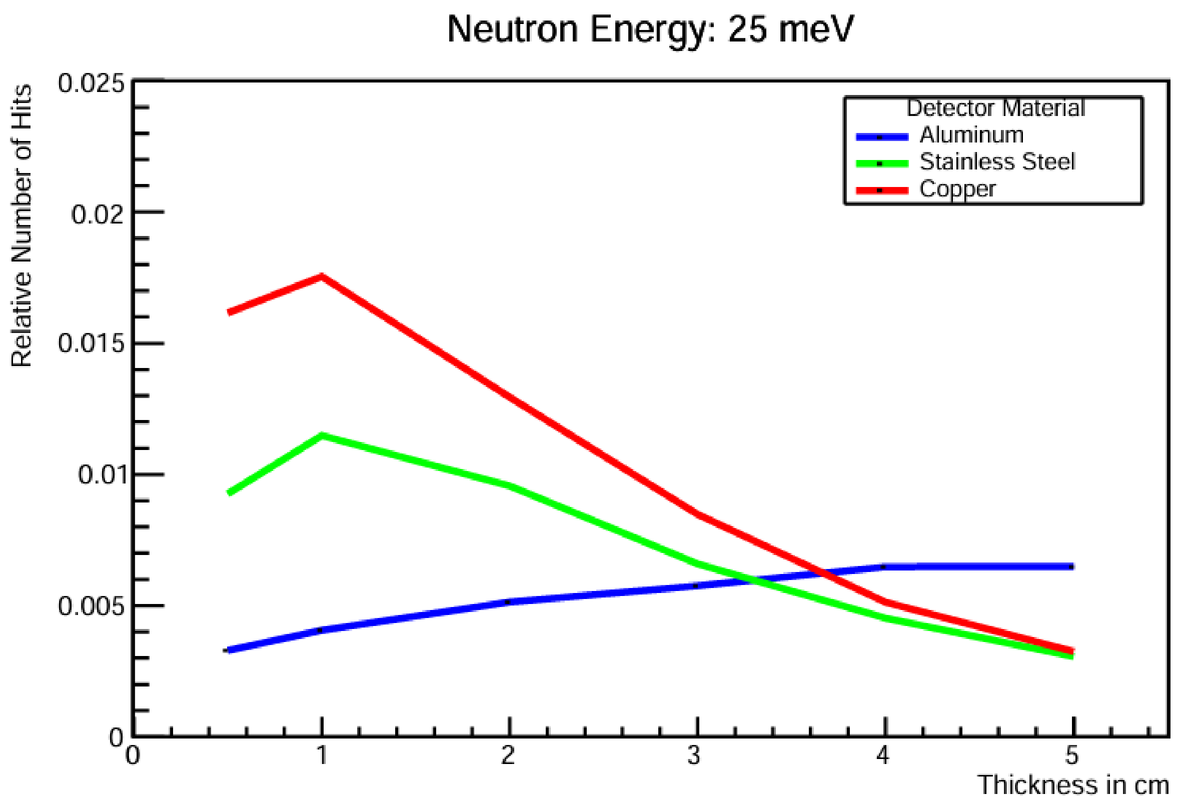

Neutron Scattering in SPCs

How can position reconstruction be performed in a scintillator detector system?

Application of detection of scattered particles in the SPC?

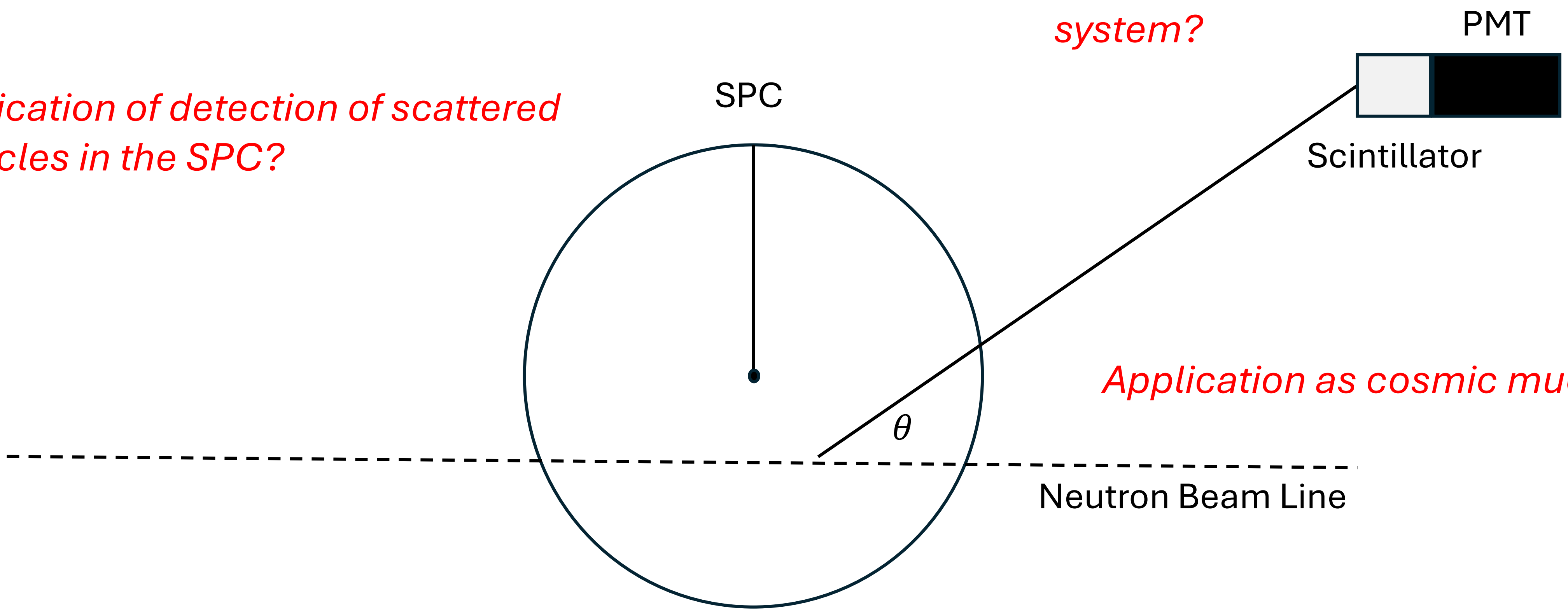

Application as cosmic muon veto?

Scintillators

- Large scintillator read-out by 4 PMTs (one at each corner)

<u>Large Scintillator:</u>
117 cm x 121 cm x 2.5 cm

<u>4 Slab Scintillators:</u>
100 cm x 40 cm x 1.5 cm

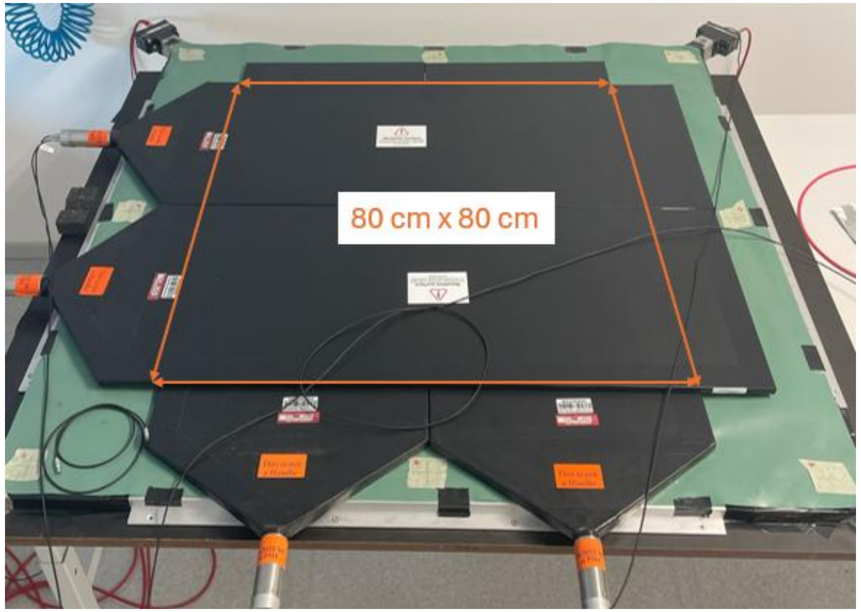

<u>2 Hodoscope Scintillators:</u>
3.7 cm x 28 cm x 1 cm

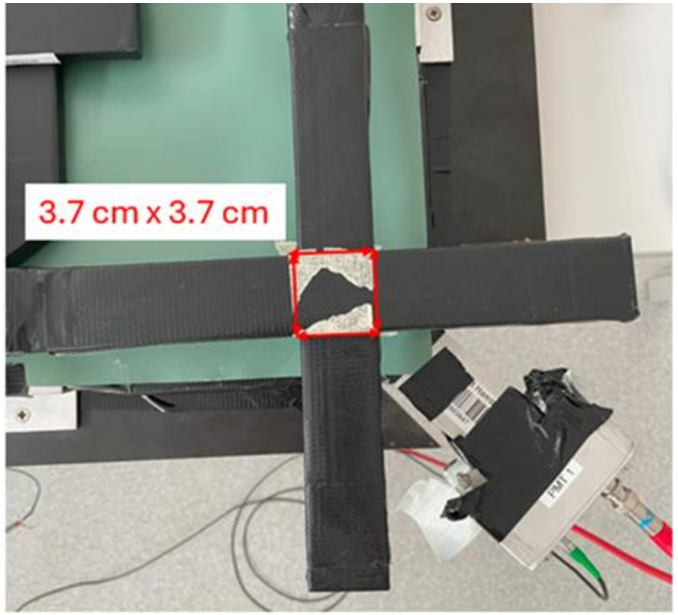

Characterization of the Scintillator System

- Determination of PMT operation voltage
- Efficiency of cosmic muon detection :
  - Online: Using NIM units (Discriminators and Majority Coincidence), evaluated using Pass-Fail test in the oscilloscope
  - Offline: Event recording with oscilloscope, evaluated with offline analysis
- Position reconstruction using least squares fit
- Determination of the fake rate

PMT Operation Voltage Determination

- Detection of cosmic muons

<u>Large scintillator:</u>

- 40 cm x 40 cm area in the center as trigger (operated at 850 V)
- Pass-Fail Test for a range of voltages from 700 V to 1130 V

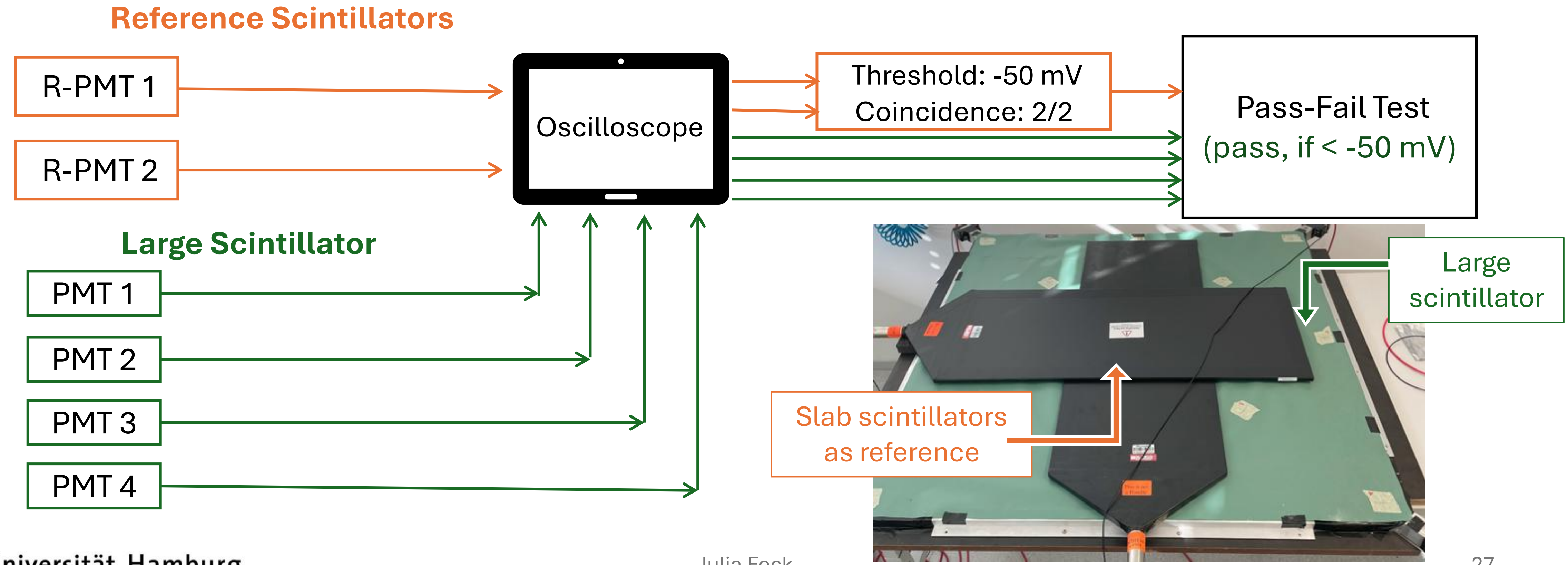

Universität Hamburg
DER FORSCHUNG | DER LEHRE | DER BILDUNG

PMT Operation Voltage Determination

- Detection of cosmic muons

<u>Large scintillator:</u>

- 40 cm x 40 cm area in the center as trigger (operated at 850 V)
- Pass-Fail Test for a range of voltages from 700 V to 1130 V

<u>Slab scintillators:</u>

- Measurement in 2 parts, using S1 and S3 as trigger and vice versa
- Problem with Slab 3 and Slab 4
- Voltage scan was only performed after the incident

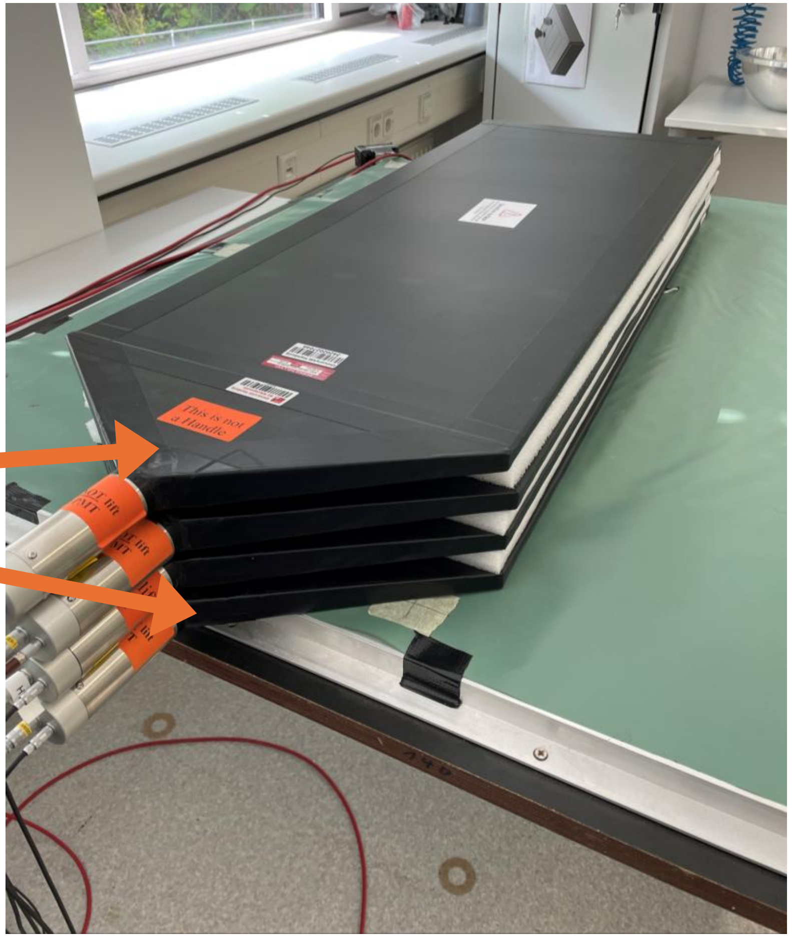

PMT Operation Voltage Determination

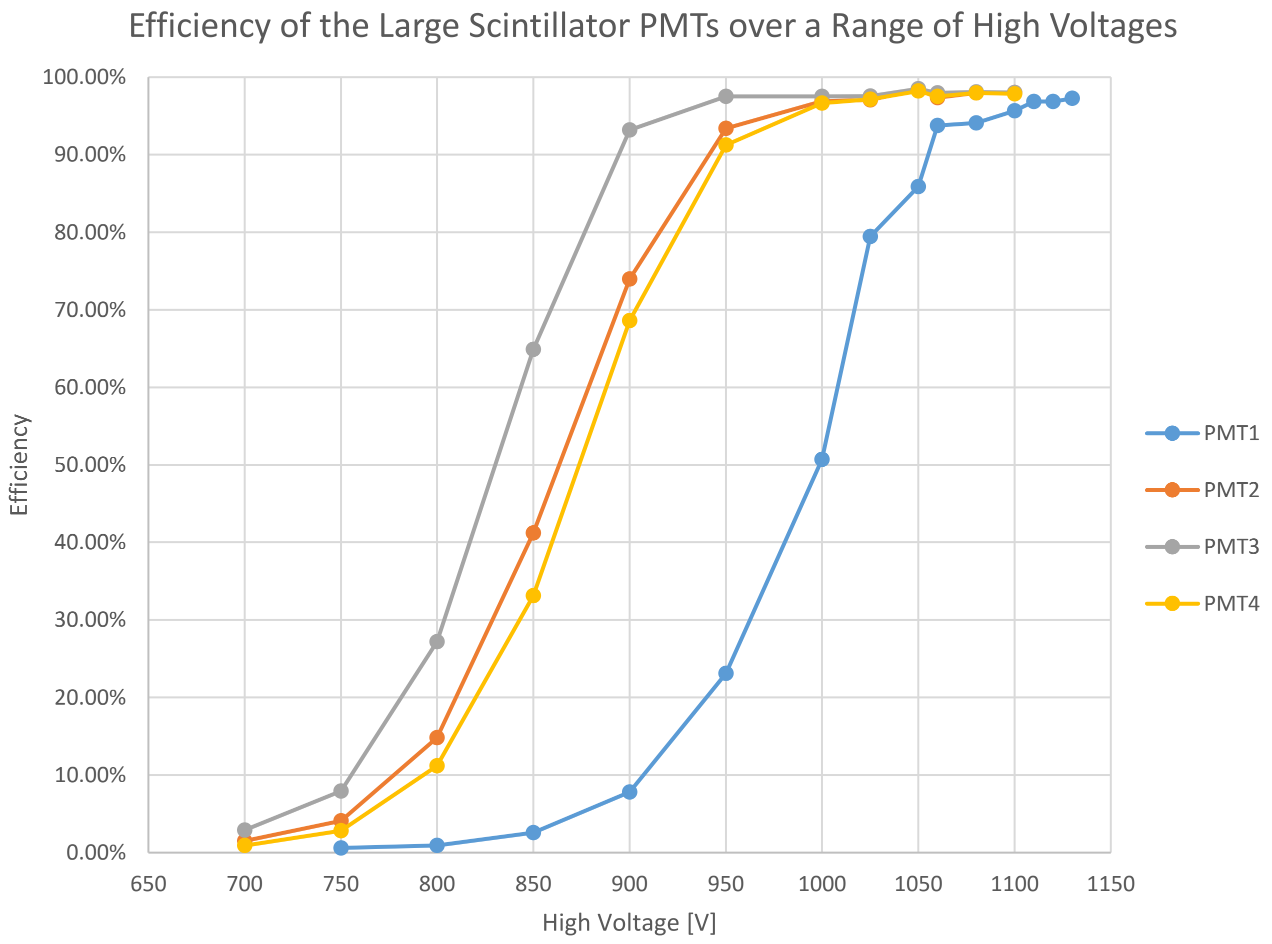

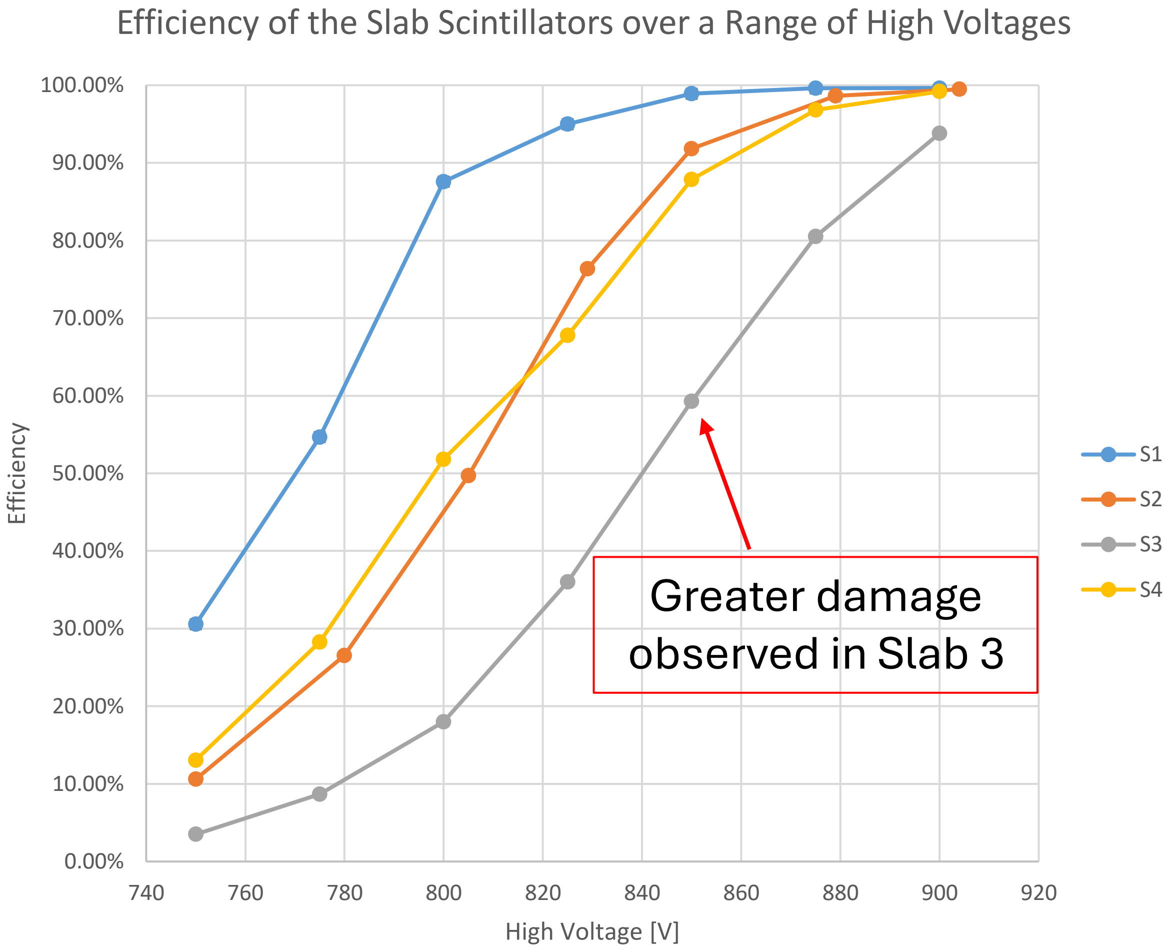

PMT Operation Voltage Determination

PMT	Voltage [V]	Efficiency [%]
Large Scintillator		
PMT 1	1100	96.9±0.4
PMT 2	1050	98.4±0.4
PMT 3	980	97.5±0.5
PMT 4	1050	98.2±0.4
Slab Scintillator		
Slab 1	850	98.90±0.15
Slab 2	850	91.84±0.39
Slab 3	850	59.29±0.69
Slab 4	850	87.88±0.46

Online Efficiency Measurement per PMT

- Threshold : -50mV

	Efficiency Center [%]	Efficiency Near PMT 4 [%]	Efficiency Near PMT 3 [%]
PMT 1	97.68±0.22	97.52±0.22	97.34±0.23
PMT 2	97.80±0.21	97.62±0.22	97.44±0.22
PMT 3	97.90±0.20	97.76±0.21	97.66±0.21
PMT 4	98.02±0.20	97.90±0.20	97.74±0.21
$p(\geq 3)$	99.73±0.03	99.69±0.03	99.65±0.03

Pretty homogenic around 99.7 %

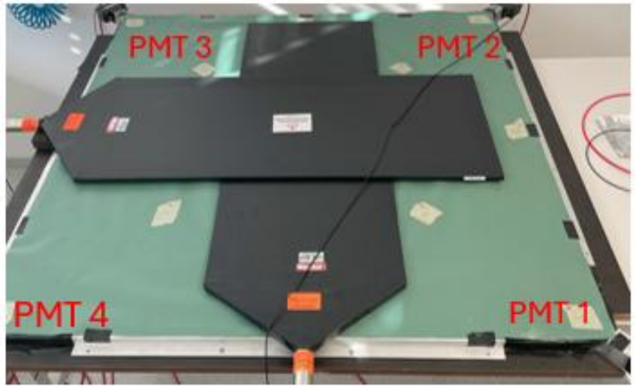

Measurement in the center position

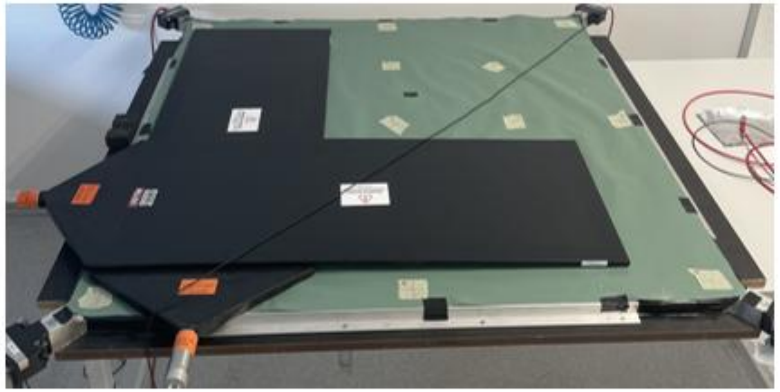

Measurement close to PMT4

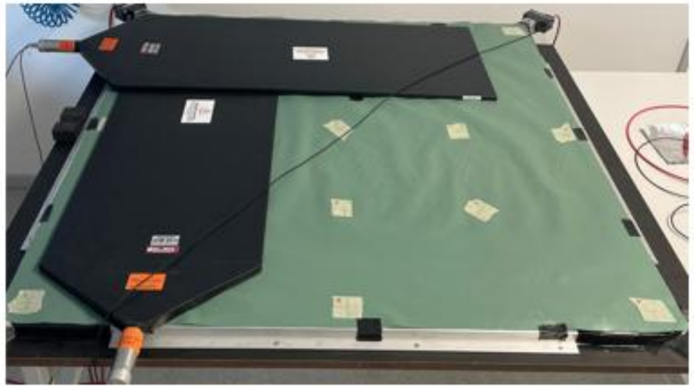

Measurement close to PMT3

Online Efficiency Measurement using NIM Units

- Discriminator with adjustable threshold and logic pulse width
- Majority coincidence with $\geq 1, \geq 2, \geq 3, \geq 4$ conditions

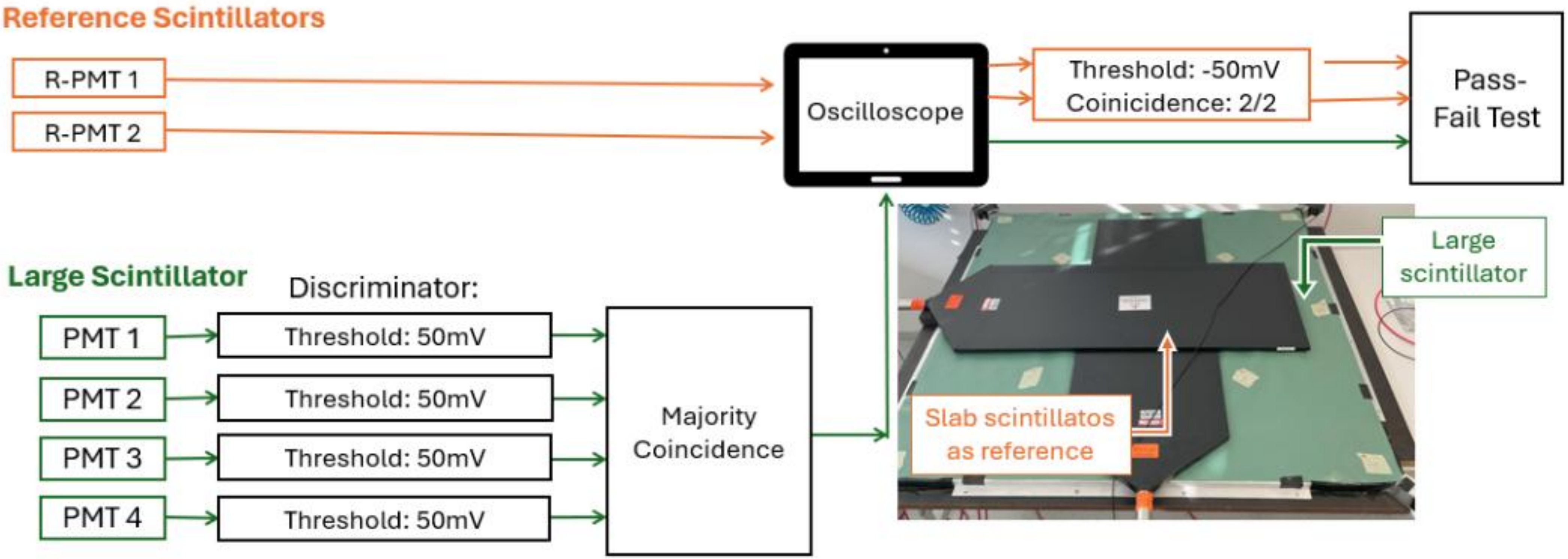

Online Efficiency Measurement

Does not match calculated 99.7%

40 cm x 40 cm area at different measurement positions (50 mV threshold):

	Efficiency Center[%]	Efficiency Near PMT 4 [%]	Efficiency Near PMT 3 [%]
$p(\geq 3)$	97.76±0.21	97.20±0.23	97.08±0.24

Global efficiency measurement (80 cm x 80 cm):

Coincidence	Efficiency for -50 mV Threshold [%]	Efficiency for -80 mV Threshold [%]
≥ 1	97.5±0.4	97.6±0.2
≥ 2	97.4±0.3	97.6±0.2
≥ 3	97.3±0.3	96.0±0.3
≥ 4	96.9±0.3	87.7±0.5

- May be due to the coincidence NIM unit, which has shown erratic behaviour
- Under investigation

Local offline efficiency measurement

- Measurements at different scintillator positions with hodoscope scintillators

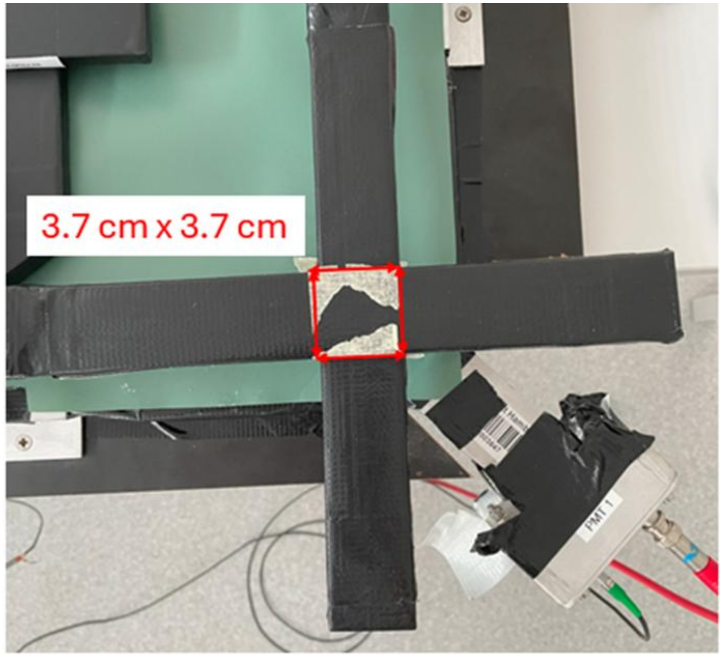

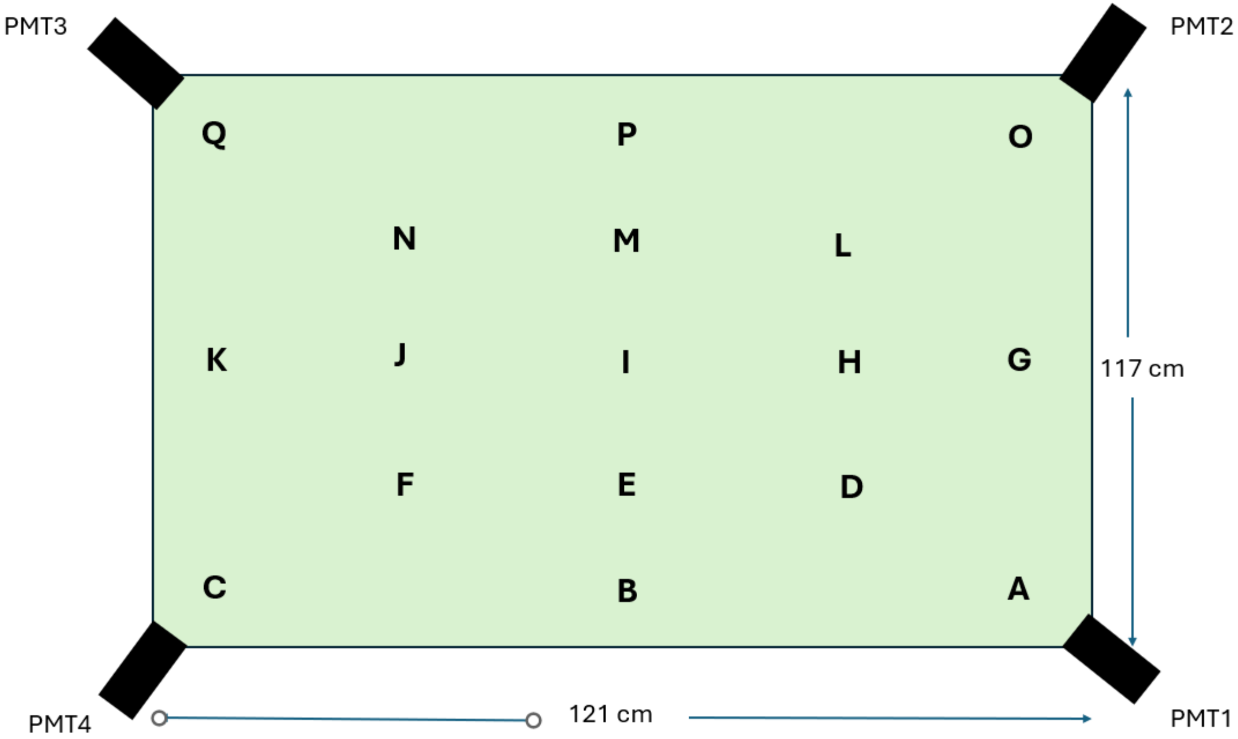

Local offline efficiency measurement

Waveforms:

- Signal of each PMT (pulse height)
- Dashed line: “charge“ (integral of pulse height)

Efficiency determination:

- Baseline correction for the pulse height
- Pulse height threshold: -30 mV
- “Charge“ threshold: -50 mV
- Counting how many PMTs had signal over threshold (similar to coincidence)

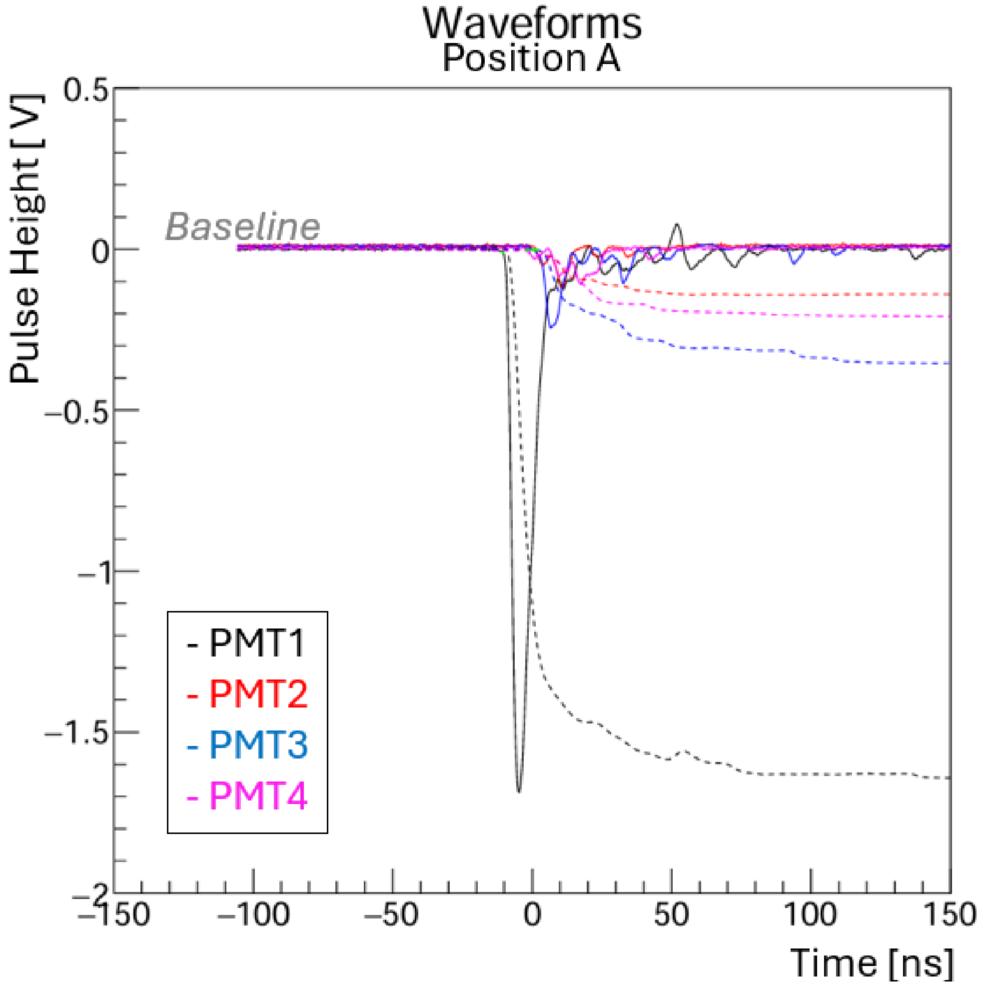

Local offline efficiency measurement

Efficiencies for 3 or 4 coincidences:

Pulse Height Threshold: <-30 mV

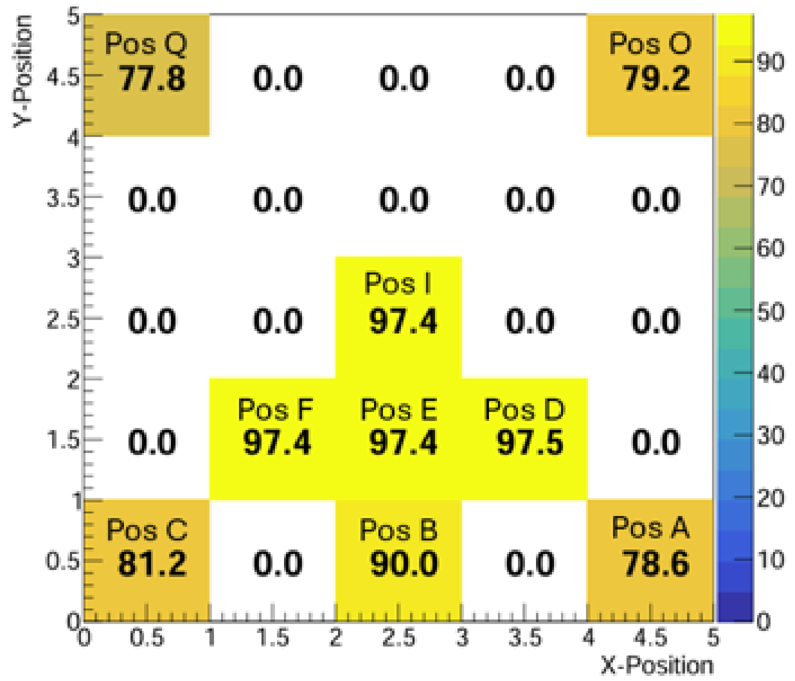

Charge Threshold: <-50 mV

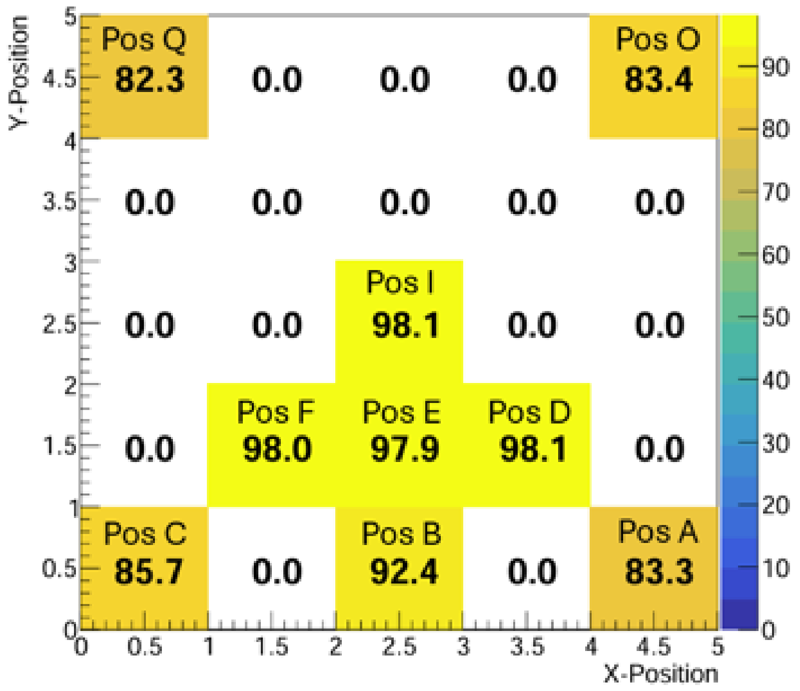

- Uncertainties ~ 0.2 % to 0.5 %

Local offline efficiency measurement

Efficiencies for 3 or 4 coincidences:

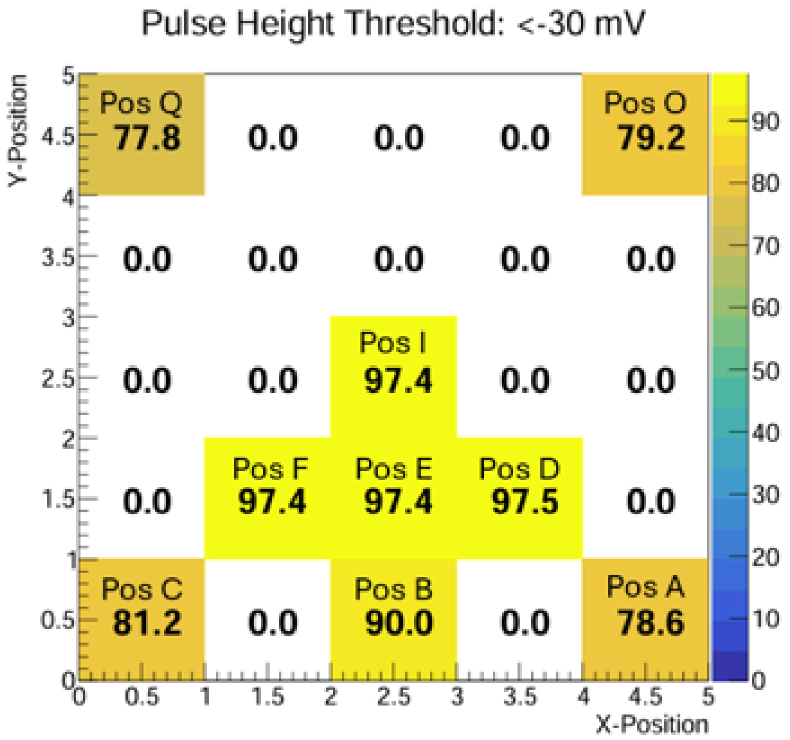

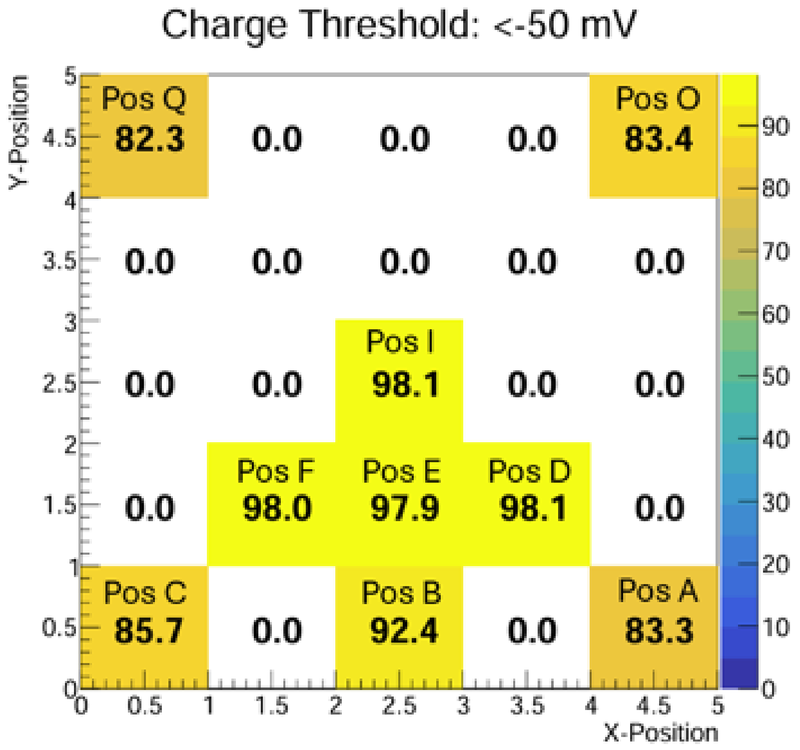

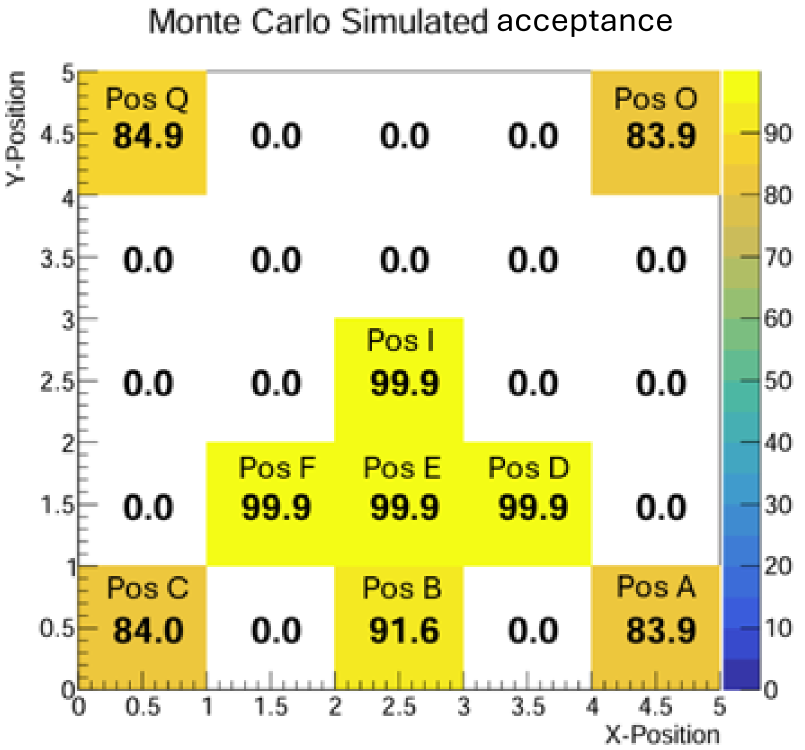

- Uncertainties ~ 0.2 % to 0.5 %
- Monte Calo simulation of the experimental setup (acceptance only due to geometrical effects)

Local offline efficiency measurement

Monte Carlo corrected efficiencies for 3 or 4 coincidences:

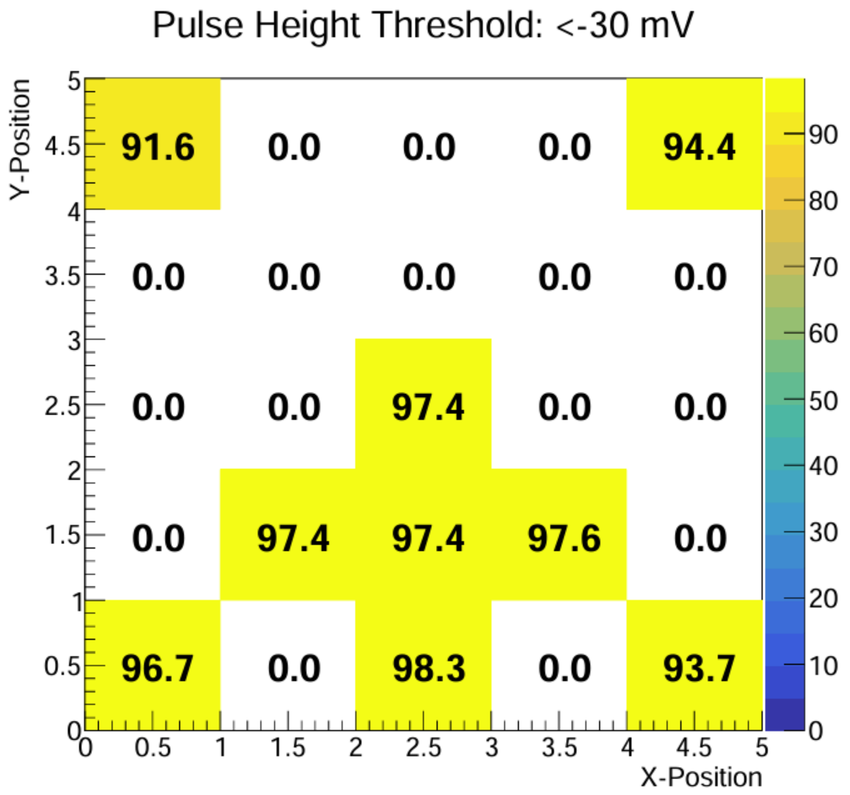

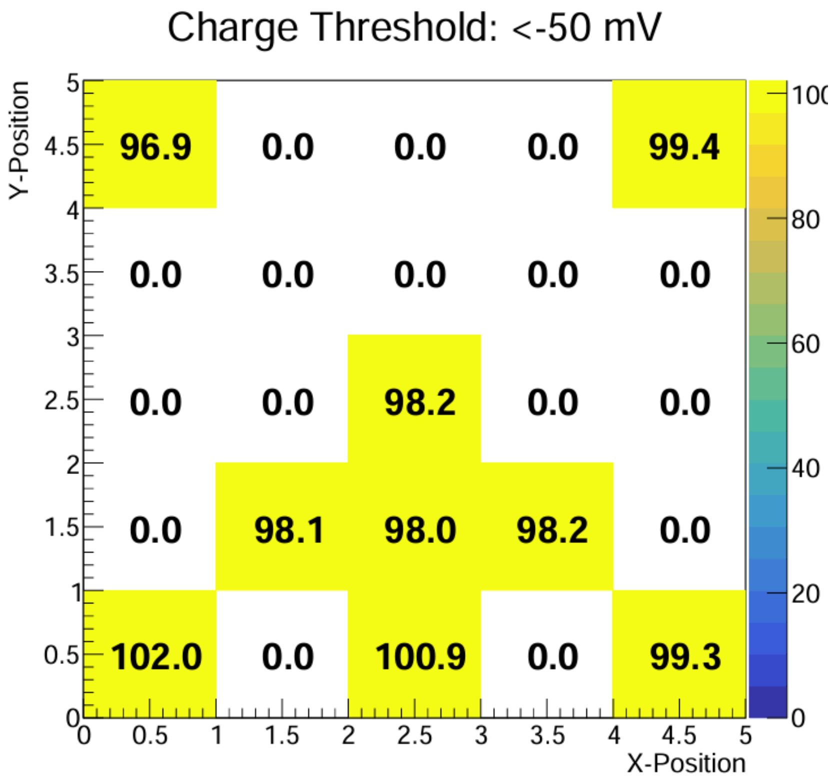

The efficiency over 100 % arises from the correction with the Monte Carlo acceptance and is due to the statistics

Position Reconstruction

- No absolute time stamp, analysis of time differences
- Time: $baseline - 5 \cdot \sigma$
- 4/4 coincidence

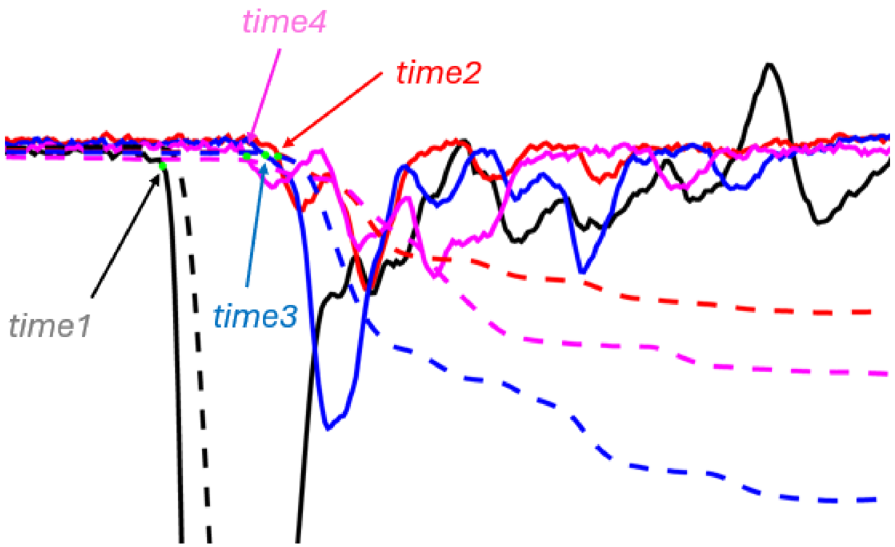

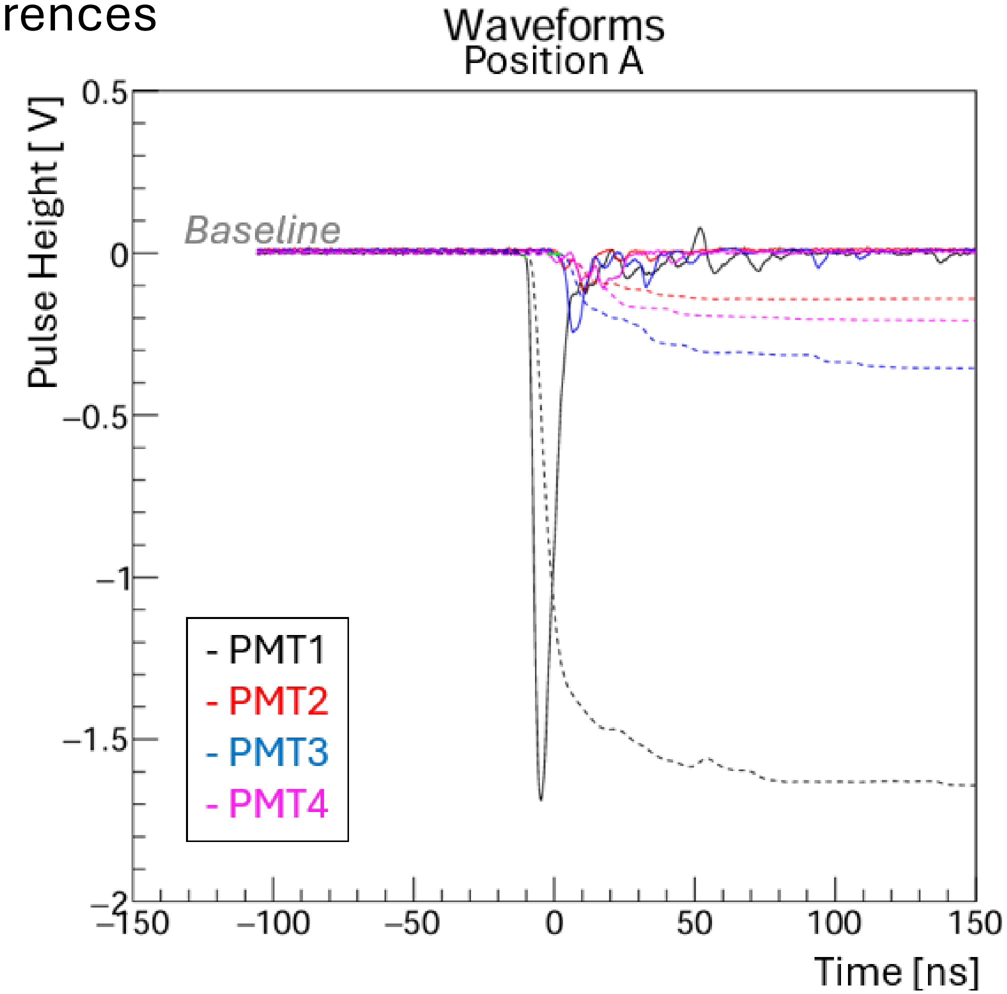

Universität Hamburg
DER FORSCHUNG | DER LEHRE | DER BILDUNG

Position Reconstruction

- No absolute time stamp, analysis of time differences
- Time: $baseline - 5 \cdot \sigma$
- 4/4 coincidence

<u>Determination of the speed of light</u>

- Data from the corner positions
- Time differences between diagonal PMTs
- $c_{measred} = 16.5 \pm 1.4$ cm/ns $(c_{theo} = 19\ cm/ns)$

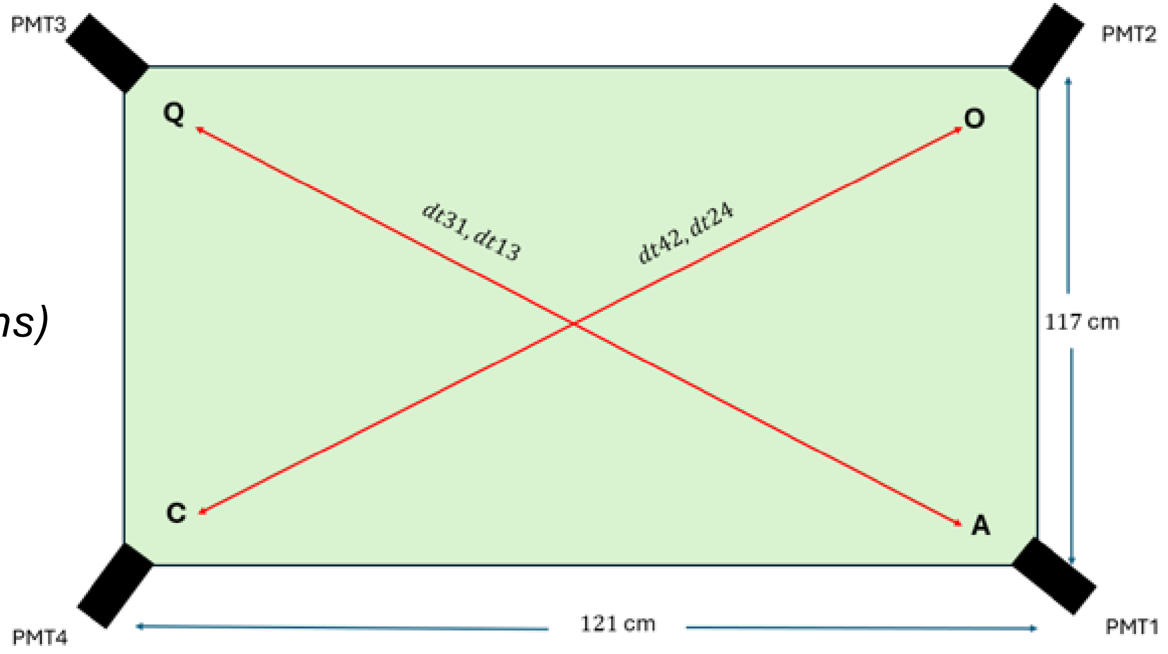

Universität Hamburg
DER FORSCHUNG | DER LEHRE | DER BILDUNG

Position Reconstruction

- $c_{measred} = 16.5 \pm 1.4$ cm/ns $(c_{theo} = 19\ cm/ns)$
- Coordinate system with 120 x 120 bins
- Comparison of calculated and measured time difference for each bin
- Square (x,y) that gives the value closest to zero -> most likely incident muon position

$$s_1 = \sqrt{(x - L_x)^2 + y^2}$$

$$s_2 = \sqrt{(x - L_x)^2 + (y - L_y)^2}$$

$$s_3 = \sqrt{x^2 + (y - L_y)^2}$$

$$s_4 = \sqrt{x^2 + y^2}$$

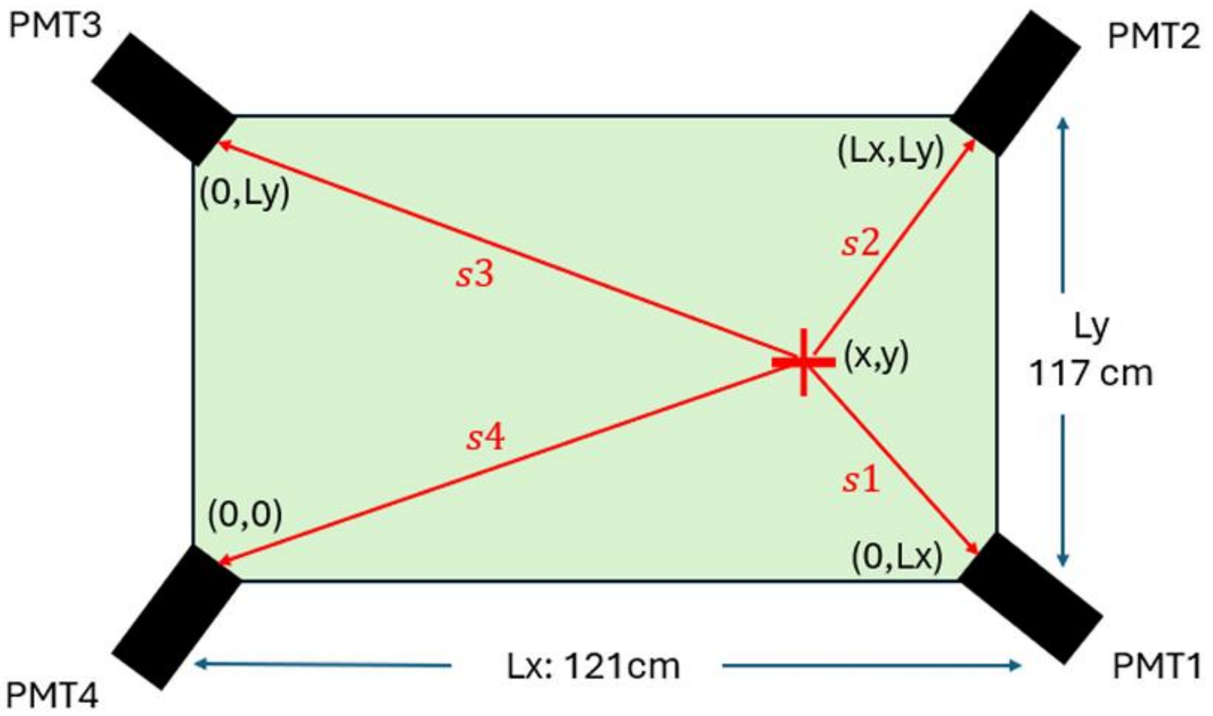

Position Reconstruction

- Best-fit positions for all events
- $\delta_{x,Scint} = 10.38 \pm 0.11\mathrm{cm}$, $\delta_{y,Scint} = 11.16 \pm 0.11\mathrm{cm}$

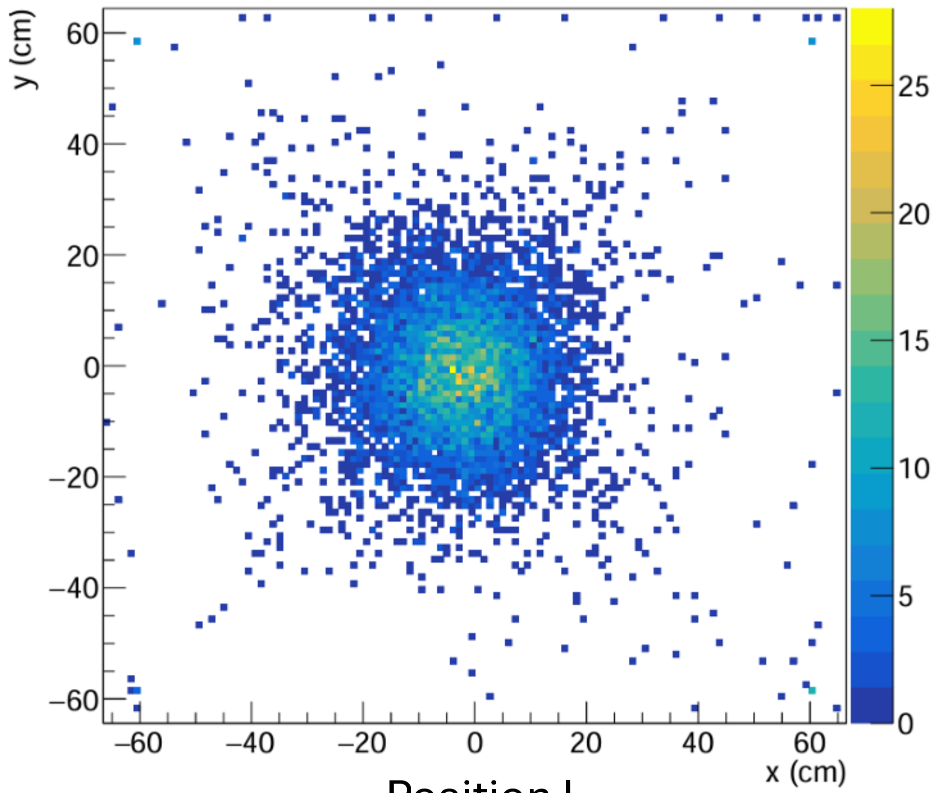

Position I

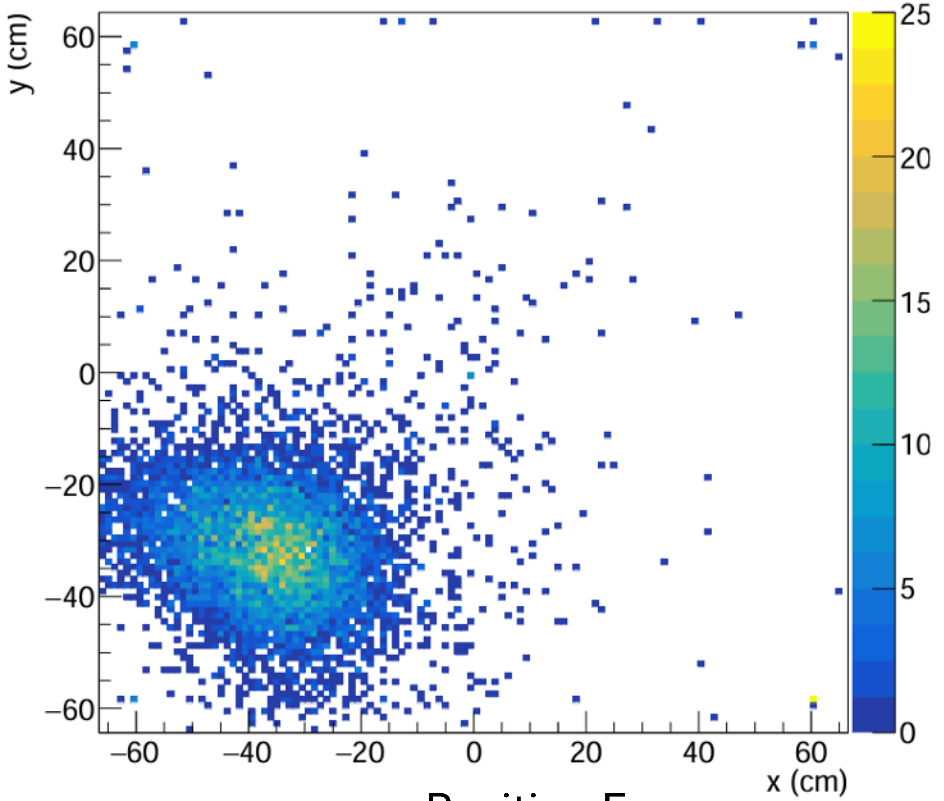

Position F

Measurement of the Fake Rate

- Measurement of the muon rate with NIM units

<u>Slab scintillator system as reference:</u>

- 50 mV threshold
- Measured rate: $0.64\ /cm^2\ /min$
- Efficiency corrected rate: $0.70\ /cm^2\ /min$

➢ Slab scintillator system: possible option as veto

➢ Large scintillator: Cosmic muon rate is higher than reference indicating fake rate, especially for looser coincidence requirements and lower threshold

<u>Large scintillator:</u>

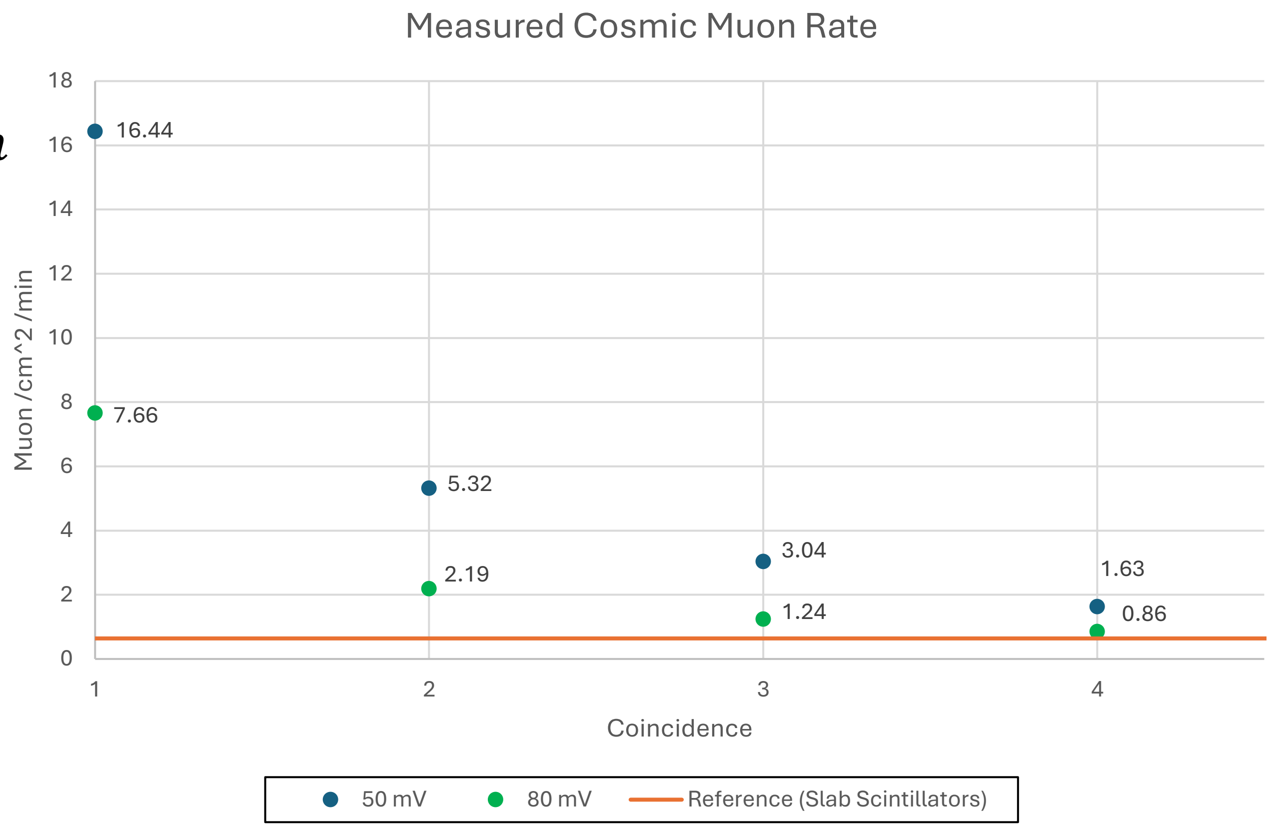

Summary

Uncertainty of the nuclear recoil energy:

- Depends strongly on position resolution of the scintillator and spread of the neutron beam
- Heavier gases result in larger scattering angles -> better energy resolution
- Greater distances from the backing detector to the SPC improves energy resolution

Conceptual design of a neutron scattering experiment:

- Thermal neutrons undergo neutron capture interactions in the shell ->absorption effects
- Aluminum enables neutrons to interact mostly in the gas due to low cross-section
- Sphere thickness shields neutrons from interacting in the sphere except for thermal neutrons and aluminum sphere

Characterization of a scintillator detector system:

- Efficiency is determined via various methods:
  - 97.4 ± 0.2 % (Pulse heigh threshold: -30 mV)
- Position resolution: $\delta_{x,Scint} = 10.38 \pm 0.11$ cm , $\delta_{y,Scint} = 11.16 \pm 0.11$ cm
- Cosmic muon rate of the slab scintillator: $0.70\ /cm^2\ /min$ (-50 mV threshold)
- Cosmic muon rate of the large scintillator: $0.86\ /cm^2\ /min$ (-80 mV threshold, 4/4 coincidence)

Back Up

Summary

Efficiencies for 3 or 4 coincidences signal over threshold

Global efficiency measured online:

- Calculated via the individual efficiencies of the PMTs:
  99.76 ± 0.03 % (-50 mV threshold)
- Measured with the majority coincidence:
  97.3 ± 0.3 % (-50 mV threshold)

Local efficiency determined offline (Monte Carlo corrected):

- Pulse heigh threshold: -30 mV
  97.4 ± 0.2 % (center position)
- Charge threshold: -50 mV
  98.2 ± 0.2 % (center position)

Large Scintillator:
1.17 m x 1.21 m

Determination of the fake rate

- Reference scintillator: $0.70\ /cm^2\ /min$ (-50 mV threshold)
- Large scintillator: $0.86\ /cm^2\ /min$ (-80 mV threshold, 4/4 coincidence)

Determination of the Fake Rate

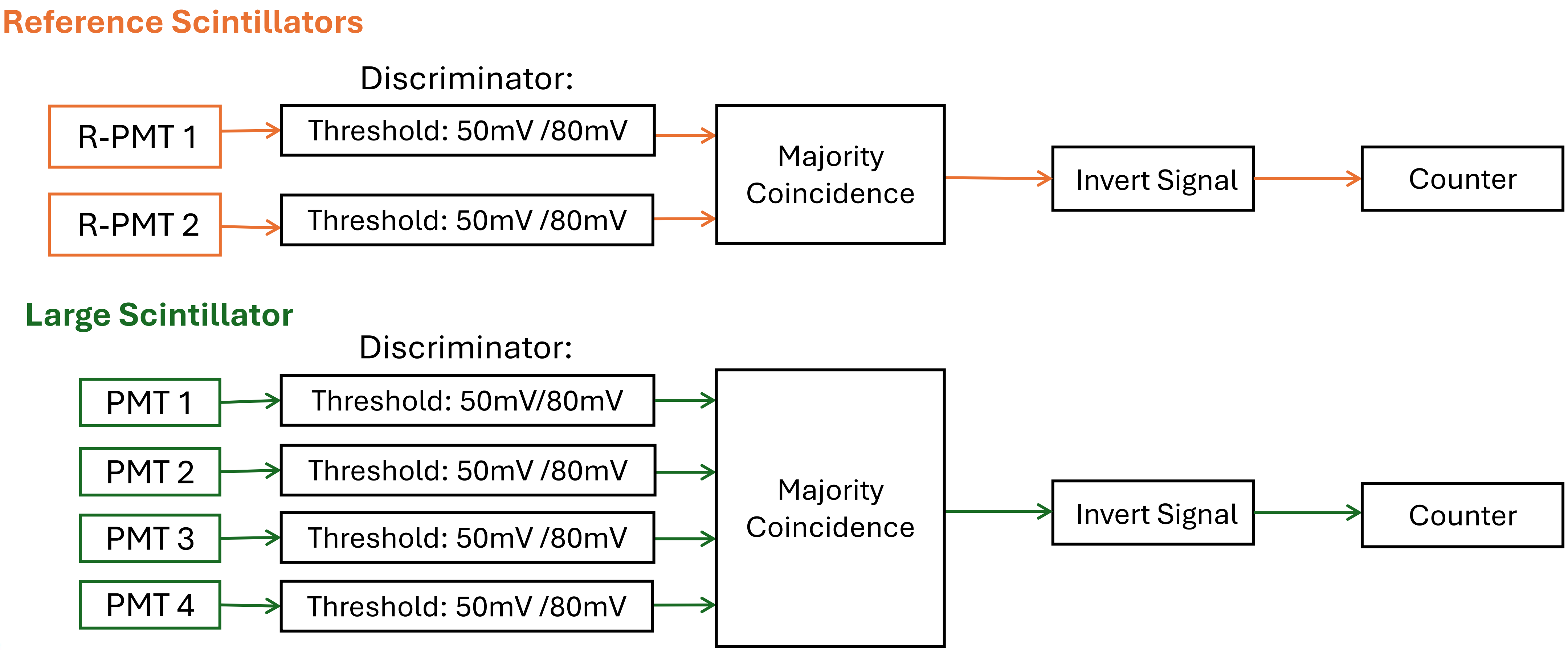

Global online efficiency measurement